

# Journal of Visualized Experiments

## Automating Aggregate Quantification in Caenorhabditis elegans

--Manuscript Draft--

<b>Article Type:</b>	Invited Methods Article - JoVE Produced Video
<b>Manuscript Number:</b>	JoVE62997R1
<b>Full Title:</b>	Automating Aggregate Quantification in Caenorhabditis elegans
<b>Corresponding Author:</b>	Daniel M Czyz University of Florida Gainesville, Florida UNITED STATES
<b>Corresponding Author's Institution:</b>	University of Florida
<b>Corresponding Author E-Mail:</b>	dczyz@ufl.edu
<b>Order of Authors:</b>	Alfonso Vaziryan-Sani Robert Handy Alyssa Walker Carol Navya Pagolu Samantha Enslow Daniel M Czyz
<b>Additional Information:</b>	
<b>Question</b>	<b>Response</b>
Please specify the section of the submitted manuscript.	Biology
Please indicate whether this article will be Standard Access or Open Access.	Open Access (\$3900)
Please indicate the <b>city, state/province, and country</b> where this article will be <b>filmed</b> . Please do not use abbreviations.	Gainesville, Florida, USA
Please confirm that you have read and agree to the terms and conditions of the author license agreement that applies below:	I agree to the <a href="#">Author License Agreement</a>
Please provide any comments to the journal here.	
Please confirm that you have read and agree to the terms and conditions of the video release that applies below:	I agree to the <a href="#">Video Release</a>

**TITLE:**

Automating Aggregate Quantification in *Caenorhabditis elegans*

**AUTHORS AND AFFILIATIONS:**

Alfonso S. Vaziriyani-Sani<sup>1</sup>, Robert D. Handy<sup>1</sup>, Alyssa C. Walker<sup>1</sup>, Carol Navya Pagolu<sup>1,2</sup>, Samantha M. Enslow<sup>1</sup>, Daniel M. Czyż<sup>1</sup>

<sup>1</sup>Department of Microbiology and Cell Science, University of Florida, Gainesville, Florida, USA

<sup>2</sup>Department of Computer and Information Science and Engineering, University of Florida, Gainesville, Florida, USA

**Email addresses of co-authors:**

Alfonso S. Vaziriyani-Sani	(alfonso452@ufl.edu)
Robert D. Handy	(handyrobert@ufl.edu)
Alyssa C. Walker	(awalk1@ufl.edu)
Carol Navya Pagolu	(cpagolu@ufl.edu)
Samantha M. Enslow	(samanthaenslow@ufl.edu)
Daniel M. Czyż	(dczyz@ufl.edu)

**Corresponding author:**

Daniel M. Czyż (dczyz@ufl.edu)

**KEYWORDS:**

*C. elegans*, proteostasis, polyglutamine, aggregation

**SUMMARY:**

The following protocol describes the development and optimization of a high-throughput workflow for worm culturing, fluorescence imaging, and automated image processing to quantify polyglutamine aggregates as an assessment of changes in proteostasis.

**ABSTRACT:**

A rise in the prevalence of neurodegenerative protein conformational diseases (PCDs) has fostered a great interest in this subject over the years. This increased attention has called for the diversification and improvement of animal models capable of reproducing disease phenotypes observed in humans with PCDs. Though murine models have proven invaluable, they are expensive and are associated with laborious, low-throughput methods. Use of the *Caenorhabditis elegans* nematode model to study PCDs has been justified by their relative ease of maintenance, low cost, and rapid generation time, which allow for high-throughput applications. Additionally, high conservation between the *C. elegans* and human genomes makes this model an invaluable discovery tool. Nematodes that express fluorescently tagged tissue-specific polyglutamine (polyQ) tracts exhibit age- and polyQ length-dependent aggregation characterized by fluorescent foci. Such reporters are often employed as proxies to monitor

changes in proteostasis across tissues. Manual aggregate quantification is time-consuming, limiting the experimental throughput. Furthermore, manual foci quantification can introduce bias, as aggregate identification can be highly subjective. Herein, a pipeline consisting of worm culturing, image acquisition, and data processing was standardized to support high-throughput aggregate quantification using *C. elegans* that express intestine-specific polyQ. By implementing a *C. elegans*-based image processing pipeline using CellProfiler, an image analysis software, this method has been optimized to separate and identify individual worms and enumerate their respective aggregates. Though the concept of automation is not entirely unique, the need to standardize such procedures for reproducibility, elimination of bias from manual counting, and increase throughput is high. It is anticipated that these methods can drastically simplify the screening process of large bacterial, genomic, or drug libraries using the *C. elegans* model.

## INTRODUCTION:

Age-dependent neurodegenerative protein conformational diseases (PCDs) such as Alzheimer's, Parkinson's, and Huntington's diseases, or amyotrophic lateral sclerosis, are characterized by protein misfolding that leads to aggregation, cell death, and tissue degeneration<sup>1</sup>. While protein misfolding is recognized as the culprit, the etiology of these diseases is not clear. As such, the development of effective therapies has been hindered by the lack of knowledge regarding the factors and conditions that contribute to disease onset and progression. Recent studies suggest that changes in the microbiome influence the onset, progression, and severity of PCDs<sup>2-4</sup>. However, the complexity of the human, or even murine, microbiome makes it difficult to conduct studies that would reveal the exact influence of microbes on their host. Therefore, simpler organisms, such as *Caenorhabditis elegans*, are often used as a discovery tool<sup>5-8</sup>. Recent studies have employed *C. elegans* to investigate the effect of bacteria on host proteostasis and disease pathogenesis<sup>9,10</sup>. Bacterial colonization, hormesis, and genomic changes are among exemplar conditions that affect the aggregation of polyglutamine (polyQ) tracts<sup>9,11,12</sup>. Additionally, these misfolded protein clusters exhibit polyQ-length and age-dependent accumulation within the host and are associated with impaired motility<sup>9,13</sup>. The relatively simple approach of quantifying fluorescently labeled puncta can generate important data on conditions, factors, or drugs that affect protein folding and aggregation.

Though quantification of fluorescent puncta has proven to be a reliable and relatively simple procedure, the challenge remains to develop a protocol that would facilitate large-scale screening of compounds, bacteria, or conditions that affect protein aggregation. The concept of automated *C. elegans* image processing and puncta quantification is not entirely novel, as a number of practical support tools have been developed<sup>14,15</sup>. However, the integration of culturing, image acquisition, and a processing pipeline are essential in eliminating variability in results and allowing for higher-throughput screens.

As such, the intent of this manuscript is to standardize the procedure used to quantify polyQ aggregation in *C. elegans* as a proxy to detect changes in proteostasis. This task was accomplished

by employing CellProfiler, an open-source image analysis software<sup>16</sup> capable of automated worm and aggregate identification, and is integrated into a larger protocol for culturing worms, acquiring images, and processing data.

## **PROTOCOL:**

All procedures followed the safety guidelines that were reviewed and approved by the Institutional Biosafety Committee of the University of Florida. Appropriate waste biosafety measures were taken to mitigate the risk of exposure to Biological Safety Level-2 bacteria.

NOTE: For all experiments, *C. elegans* must be propagated and maintained on nematode growth media (NGM) plates seeded with *Escherichia coli* OP50.

### **1. Preparation of 10 cm NGM plates**

1.1. Combine 3 g of NaCl, 2.5 g of trypticase-peptone, and 17 g of agar into a 2 L flask, and fill to 1 L with double distilled water (ddH<sub>2</sub>O). Add magnetic stir bar prior to autoclaving.

1.2. Autoclave the mixture for 45 min at 121 °C and a pressure of 21 psi. Let the mixture cool to 50 °C in a water bath.

1.3. Using aseptic techniques, add the following solutions: 1 mL of 1 M CaCl<sub>2</sub>·2H<sub>2</sub>O, 1 mL of 1M MgSO<sub>4</sub>·7H<sub>2</sub>O, 1 mL of 5 mg/mL cholesterol dissolved in 100% ethanol (warmed to room temperature), and 25 mL of 1 M KH<sub>2</sub>PO<sub>4</sub> (pH = 6.0). Mix using a magnetic stir plate. Mixing may be performed for 1 min at 700 RPM.

1.4. Pour approximately 20 mL of the mixture per 10 cm plate. Pour until mixture gradually fills the entire bottom. Alternatively, a graduated serological pipette can also be used.

1.5. Allow the plates to dry for 24 h at room temperature prior to seeding with bacteria or store the plain plates at 4 °C after drying.

NOTE: All media components are handled using aseptic techniques. Steps 1.3–1.4 should be performed in a laminar flow hood.

### **2. Preparation of NGM agar with FUDR in 24-well plates**

2.1. Follow steps 1.1–1.3.

2.2. Supplement NGM with 5-Fluoro-2'-deoxyuridine (FUDR) and mix to achieve a final concentration of 100 µg/mL.



NOTE: FUDR inhibits DNA replication and, as a result, blocks *C. elegans* reproduction by targeting germline and embryogenesis, ultimately affecting lifespan. Therefore, it is important to allow worms to fully develop into young adults before transferring onto FUDR-containing plates.

CAUTION: FUDR is toxic and should be handled according to the manufacturer's Material Safety Data Sheet.

2.3. Using a pipette gun, dispense 1 mL of NGM-FUDR into each well.

NOTE: This process can be facilitated by the use of an automated plate pouring system.

2.4. Let it sit for 24 h at room temperature prior to seeding with bacteria or storing plain plates at 4 °C after drying.

### **3. Seeding of plates: OP50 and additional test bacteria**

3.1. To prepare an overnight *E. coli* OP50 culture, add a 200 µL of a bacterial aliquot from a frozen stock into a 500 mL Erlenmeyer flask containing 250 mL of fresh and sterile Luria broth (LB).

NOTE: The volume of the media depends on the number of plates that need to be seeded. To prepare other bacterial cultures, inoculate a 16-mL culture tube containing 5 mL of growth medium with bacteria from frozen stock using a sterile micropipette tip.

3.2. Incubate overnight in a 37 °C incubator, shaking at 220 RPM (rotations per minute).

NOTE: Use sterilized flasks with at least twice the working volume of media and seal with aluminum foil. Perform the inoculation step and bacterial dispensing using aseptic techniques.

3.3. Dispense 1–2 mL of the overnight *E. coli* OP50 culture onto the center of each 10 cm NGM plate. This culture does not need to be spread around the NGM plate.

3.4. Allow the plates to dry at room temperature prior to use/storage.

NOTE: Seeded plates with lids on can be placed in a hood with airflow to facilitate drying.

### **4. Culturing and seeding of plates: 24-well plates**

4.1. Prepare an overnight culture of desired bacterial strains, adhering to culturing instructions found in steps 3.1–3.2.

4.2. Transfer 200  $\mu$ L of each bacterial culture into each well of a 24-well plate containing NGM agar. A 200  $\mu$ L volume of bacteria will cover the entire agar area, maximizing the amount of food to ensure that worms will not avoid the bacterial lawn.

4.3. Leave the plates cracked open in a biological safety cabinet (BSC) to facilitate drying. Check the plates periodically to prevent excessive dehydration and change plate orientation for promoting even airflow and drying. The plates should dry within 5 h.

NOTE: Any work with Biological Safety Level-2 bacteria must be performed in certified BSCs and approved by the Institutional Biosafety Committee.

## 5. Age synchronization

NOTE: All steps should be performed using proper aseptic techniques (i.e., working close to a flame or inside a BSC).

5.1. Wash gravid hermaphrodites off 10 cm OP50 plates using filter-sterilized M9 solution (5.8 g of  $\text{Na}_2\text{HPO}_4 \cdot 7\text{H}_2\text{O}$ , 3.0 g of  $\text{KH}_2\text{PO}_4$ , 5 g of NaCl, 0.25 g of  $\text{MgSO}_4 \cdot 7\text{H}_2\text{O}$ , in 1 L of dd  $\text{H}_2\text{O}$ ).

5.1.1. Pipette M9 solution onto the plate several times using a sterile glass or plastic serological pipet to lift worms from the bacterial lawn.

5.1.2. Collect the worm suspension and transfer the solution into a 15 mL polystyrene conical tube.

5.2. Centrifuge at 270 x *g*, room temperature (RT, ~23 °C), for 2 min.

5.3. Aspirate using a vacuum trap flask and discard the supernatant, leaving the worm pellet undisturbed.

5.3.1. Resuspend the pellet in 5–10 mL of M9 to wash the worms and repeat steps 5.2–5.3 twice.

5.4. Add 5 mL of 20% bleaching solution (8.25 mL of dd $\text{H}_2\text{O}$ , 3.75 mL of 1M NaOH, 3.0 mL of non-germicidal bleach) to the tube and invert continuously to dissolve the worms. Worms are ready to centrifuge once they have almost completely dissolved.

NOTE: Bleaching times and volume of bleaching solution will depend on the size of the sample. Over and under-bleaching are common errors. As such, this process generally requires optimization to determine when the sample is ready for centrifugation.

5.5. Centrifuge for 2 min at 423 x *g* and discard the supernatant.

209 5.6. Add 10 mL of sterile M9 to resuspend the egg pellet.

210  
211 5.6.1. Centrifuge the tube for 2 min at 423 x *g* to pellet the eggs. Remove the supernatant with  
212 an aspirator flask.

213  
214 5.6.2. Repeat steps 5.6–5.6.1.

215  
216 5.7. Resuspend the egg pellet in 5 mL of sterile M9 and place it on a nutator overnight at the  
217 desired temperature.

218  
219 NOTE: Age-synchronized L1 larvae will be ready to transfer to plates the following day.

## 220 221 **6. Worm preparation post age-synchronization**

222  
223 6.1. Centrifuge the age-synchronized worms at 270 x *g* for 3 min at RT (~23 °C).

224  
225 6.2. Aspirate the supernatant in a clean environment, such as a flow hood or next to a Bunsen  
226 burner. Leave approximately 200 µL of the supernatant and resuspend the worms.

227  
228 6.3. Using a micropipette, transfer the concentrated worm suspension to 10 cm NGM plates  
229 that have been previously seeded with OP50.

230  
231 NOTE: Each plate can support 1,500 worms without running out of food; however, this  
232 concentration may require adjustment depending on the density of the bacterial lawn and  
233 growth temperature. It is recommended to use multiple plates to prevent worms from starving.  
234 It is important to note that these plates must not contain FUDR.

235  
236 6.4. Allow the plates to dry, invert, and store at 25 °C for 48 h.

237  
238 NOTE: Depending on the condition of the screen, worms from step 6.1 can be placed directly  
239 onto test plates (containing bacteria, drugs, or test compounds). If the desired test condition  
240 affects development, worms should be cultured on NGM containing OP50 until young adults (~48  
241 h) before exposing them to test conditions.

242  
243 6.5. Following the 48-h incubation, wash the worms from the plates with sterile M9 solution  
244 and place them into conical tubes.

245  
246 NOTE: Adult worms will sink to the bottom of the tube. The exact time will vary according to the  
247 number of worms recovered from 10 cm plates. Under these conditions, the worms settle down  
248 within 10 min.

6.6. Perform visual inspection to determine the duration of the settling time such that any residual eggs or hatched larvae are removed.

6.7. Add an additional 10 mL of M9 to rinse the residual bacteria from worm bodies.

6.7.1. Centrifuge the worms for 2–3 min at  $270 \times g$  at 23 °C.

6.7.2. Perform the washing step an additional 3 times. For best results, leave about 1–1.5 mL of M9 solution in the tube after the final wash.

6.7.3. Transfer 10  $\mu\text{L}$  of the worm suspension onto a glass slide and count the number of worms.

6.7.4. Adjust the worm density to approximately 150 worms per 10  $\mu\text{L}$  of M9. The concentration of worms in suspension can be adjusted by either removing or adding M9 solution after centrifugation.

6.7.5. Confirm that the desired concentration has been established by averaging counts from several different drops. It is recommended to average counts from at least three drops.

6.8. Using aseptic techniques, transfer 10  $\mu\text{L}$  of the worm suspension containing approximately 150 worms into each well of the test plate.

6.9. Inspect the wells under a microscope to ensure that each has a sufficient number of worms. Additional worms can be added prior to incubation.

6.10. Allow the plates to dry for approximately 10 min, invert, and then transfer to a 25 °C incubator for 72 h.

NOTE: The final incubation period can be adjusted to accommodate the needs of the experiment. The 72-h incubation time is sufficient to support the growth of 150 animals feeding on 200  $\mu\text{L}$  bacteria in a 24-well plate at 25 °C.

## **7. Preparing worms for imaging**

7.1. To facilitate more effective settling and minimize sample loss, immobilize the worms prior to washing to prevent swimming and sample loss during the process.

NOTE: If working with few samples, this can be achieved through exposure to levamisole (100  $\mu\text{M}$ ). However, if working with a large number of samples, worms can be immobilized by freezing. Additionally, extended freezing (18–24 h) will prevent the further development of polyQ aggregates during preparation.

291  
292 7.1.1. Place multi-well plates at -20 °C for 15–20 min or until worms no longer move.

293  
294 7.1.2. Remove the samples from the freezer and let them sit for 5 min.

295  
296 7.2. Using a micropipette, add 1 mL of M9 chilled to 4 °C to a well of interest, repeatedly press  
297 and depress the plunger 4–6 times to wash the worms in each well.

298  
299 NOTE: Sometimes, worms can stick to micropipette tips. As such, different tips should be used  
300 between each well to prevent the mixing of worms.

301  
302 7.3. Transfer the worm suspension to a microcentrifuge tube and allow the worms to sink to  
303 the bottom.

304  
305 7.4. Aspirate and discard the supernatant. Wash the sample a total of three times.

306  
307 7.5. After worms have settled to the bottom during the final wash, aspirate 500 µL, leaving  
308 500 µL to resuspend worms.

309  
310 7.6. Transfer the remaining worm suspension to a new flat-bottom 24-well plate and place it  
311 in a -20 °C freezer for 48 h.

312  
313 NOTE: Freezing worms reduces background fluorescence and allows better visualization of  
314 aggregates.

## 315 316 **8. Imaging**

317  
318 8.1. Remove the plates from the freezer and let thaw, wipe away excess condensation, and  
319 remove the lid prior to imaging.

320  
321 NOTE: The details of image capture will vary according to the equipment and software used.  
322 Protocols for this section should only serve as a guide, and modifications are to be expected. It is  
323 also required to capture images in the tiff file format.

324  
325 8.2. During image capture, use the following microscope settings: Exposure time, 500 ms; 40x  
326 magnification with 0.63x camera adapter (25.2x), GFP intensity set to 100%.

327  
328 NOTE: Various microscope configurations and systems could acquire images different from the  
329 ones provided in the results section. To achieve a more universal description of the images  
330 required, more objective details regarding images are provided. Aggregates must be between 1.0  
331 –10.0 pixels in diameter with a fluorescent intensity of 0.10–1.0 (arbitrary units, scale 0–1) to be

properly identified by the CellProfiler. The fluorescent background for these aggregate images is generally below the 0.10 threshold. For brightfield images, worm intensity ranges from 0.7–1.0 with a background intensity of 0.1–0.2. The average length of worms in brightfield images ranges from 250 pixels to 350 pixels in length from head to tail.

8.3. Adjust transmitted light controls until the worms appear brightly illuminated in comparison to the dark background. Avoid overexposure; it will increase worm appearance.

8.4. It may be necessary to alter the positions of worms within the well to prevent excessive clumping. Use a pipette tip to gently push worms into the desired position.

8.5. Set the channel to GFP to establish a focal plane for both images.

NOTE: It is essential that the focal plane be determined in the GFP channel. Any change in focus made while capturing brightfield images will result in the misalignment of aggregates and worms during image analysis.

8.6. Capture a brightfield image and immediately take its corresponding fluorescent image without disturbing the plate.

8.7. Run test images through the pipeline to determine intensity and size values for objects in the image according to the “NOTE” after step 8.2.

NOTE: CellProfiler can provide all necessary information regarding the intensity and length of objects prior to analysis.

8.8. To assess images, first, download CellProfiler<sup>17</sup>. Open the software and drag and drop images of interest into the Images box.

8.9. Click on the images in the file list to open them.

8.10. In the top left corner of the screen are several icons; use them to measure the size of the objects or magnify a specific region. Select the magnifier glass to highlight a region of interest.

8.11. Select the arrow icon to measure the length of both worms and aggregates.

8.12. Hover over the desired object to determine its intensity value which can be seen on the bottom portion of the screen.

NOTE: Since all images are taken in grayscale, all red, blue, and green pixel values will be identical.

## 9. Image analysis

9.1. To utilize the CellProfiler image analysis pipeline, name the image pairs properly. Use the following format: P1\_A01\_S1\_C1, where P1 refers to the specific plate and its respective numeric designation; “A”, refers to the row and “01” to the column; “S” refers to a specific image pair for a single well; “C” refers to the channel, where “1” is used to denote brightfield images and “2” for fluorescent images.

9.2. Download CellProfiler (version 4.1.3 or higher) from the official website<sup>17</sup>.

9.3. Download the pipeline (**Supplemental File 1**). Upload the pipeline (Pipeline) into CellProfiler by selecting **File > Import > Pipeline from File**.

NOTE: Modules 2 and 3 have been disabled as they have been deemed unnecessary. Their function can be restored if image analysis does not yield satisfactory separation and identification of worms; however, modification of the pipeline is required.

9.4. To incorporate these modules, select the boxes located to the left of each module. Rename the Input binary image for the “UntangleWorms” module to the output image from the “convertobjectstoimage” module.

9.5. An error message may appear during initial use related to Module 2. If this occurs, proceed with the analysis.

9.6. Upload a training set used to identify worms to the “UntangleWorms” module. This training set can be found in **Supplemental File 2**.

9.6.1. Select the **UntangleWorms** module to open its settings.

9.6.2. Identify **Training Set Filename** and select the upload file icon.

9.6.3. Upload **Supplemental File 2** (training set).

9.7. Upload images by selecting the **Images** module in the top left corner. Drag and drop properly named images as described in step 9.1.

9.8. Prior to analyzing images, select the desired output folder that will be used to store the results.

9.8.1. Click on the **Output Settings** button located near the bottom left-hand corner of the program.

9.8.2. Select the folder icon to the right of **Default Output** to choose the desired output location.

9.9. Select the **Analyze Images** icon to begin image analysis.

9.10. If the analysis takes too long to complete and is stuck processing a single image, it is likely due to issues from image acquisition. If this occurs, abort the run and proceed to identify the unprocessed image(s) by sorting through the output folder and noting which image names are not found.

NOTE: These images may require additional processing to remove large or intensely lit artifacts that cannot be processed by the pipeline. In some cases, these images may need to be excluded from the analysis.

9.11. Following complete analysis, the software will organize the results into an excel spreadsheet containing individual worms (column N) and their respective number of aggregates (column K).

NOTE: A successful run will produce an excel spreadsheet containing the number of aggregates per identified worm for each well. These data can be manipulated in a manner determined by the experimenter.

9.12. Download metadata organizer (Graphical User Interface) from **Supplemental File 3** (Windows) or **Supplemental File 4** (Mac) to conveniently organize data from the output CSV file from CellProfiler.

NOTE: This software does not have an official license and will not automatically be opened after downloading.

9.13. Follow steps 9.14–9.17 if using Windows OS 64-bit. The software will not work on Windows 32-bit. Follow steps 9.18–9.20 if using Mac OS. Steps 9.21–9.22 are the same for both operating systems.

9.14. For Windows OS, locate the downloaded file and extract it to the desired location.

9.15. Locate and open the extracted folder named gui\_windowsOS\_64x and launch the application by clicking on the “gui” application icon.

9.16. A prompt may open requesting permission to run. Select **More Info** and then click **Trust Anyway**.



9.17. The metadata organizer is ready to drag and drop CellProfiler output CSV files. Continue to Step 9.21.

9.18. For Mac OS, locate the downloaded file and open gui\_macOS\_64x.zip. This step should automatically extract all files.

9.19. Open the extracted folder found in “Downloads”.

9.20. Right-click on the “gui” application and select **Open**. A prompt will appear asking for permission to open due to the lack of an official license. Select **Open** and continue to step 9.21.

9.21. Click on **Upload Your Files Here** or drag and drop the desired CellProfiler CSV files.

9.22. Click the **Organize** button, which will bring the user to a new screen with a **Download Files** button. Click on the button and select the desired location to save the output file. The output file will appear as the original filename with “\_organized” extension added to the filename.

## REPRESENTATIVE RESULTS:

Described herein is a *C. elegans* workflow that includes culturing, image acquisition, and processing protocols that allow assessment of polyQ aggregation in the presence of various bacteria using a 24-well plate format as the culturing and imaging platform (**Figure 1**). This protocol can be adjusted to study the effect of bacteria, specific conditions, small molecules, drugs, or genomic manipulations on host proteostasis. The described method has been optimized using worms that constitutively express intestinal polyQ fused to a yellow fluorescent protein (*vha6p::polyQ44::YFP*); however, other models that report on proteostasis in muscle or neurons can also be used with further optimization. For example, preliminary experiments demonstrate the application of these methods in the quantification of protein aggregates in other tissues such as muscle polyQ (**Supplemental Figure 1**). However, modification to the pipeline will be required to properly adjust for aggregate size and brightness, as mentioned in section 8 NOTE.

[Place **Figure 1** here]

The initial optimization experiments revealed various difficulties associated with overcrowding due to a large number of progenies, resulting in faster food depletion. The supplementation of FUDR in NGM plates described in section 2 solved this problem (**Figure 2**). Additionally, in the presence of FUDR, worms that were fed various bacteria had a more consistent body size, which allowed more uniform and accurate worm detection.

[Place **Figure 2** here]

Background fluorescence contributed to false positive detection of polyQ aggregates. To reduce such fluorescence signal in the intestinal tract and improve automated detection of aggregates, it was necessary to freeze worms prior to imaging. Freezing worms at -20 °C for 18–48 h

significantly improved polyQ aggregate detection by eliminating background fluorescence (**Figure 3A**). The human eye is capable of differentiating between aggregates and background fluorescence; hence the manual counting before and after the freeze is the same (**Figure 3B**). However, automated counting is not as accurate, but freezing significantly improved automated counts with accuracy comparable to manual counting (**Figure 3B**).

[Place **Figure 3** here]

Inverted brightfield illumination was used to detect the whole *C. elegans* (**Figure 4A**) and GFP channel to image polyQ::YFP aggregates (**Figure 4B**). Worm detection, detangling, and aggregate quantification for each worm were done by applying an optimized CellProfiler image processing pipeline (**Supplemental File 1**), which allows obtaining the number of aggregates per individual worm (**Figure 4C-D**). To test the feasibility of this approach and the accuracy of the automated aggregate detection and quantification, worms expressing intestine-specific polyQ44::YFP were cultured and prepared for imaging according to the established protocols (sections 1–7). The number of aggregates per worm was assessed using either the automated pipeline (sections 8–9) or manual counting. Each experiment was performed in three independent trials using 90–571 worms per condition. While the average number of aggregates per intestine obtained with the two methods had no significant difference, worms in the third trial had significantly fewer aggregates when quantified using the automated approach (**Figure 5A**). The average number of aggregates from the three trials resulted in slightly, but significantly, fewer aggregates when the quantification was done using the CellProfiler pipeline (sections 8–9) (**Figure 5B**). Nonetheless, the difference between the two approaches was minimal, indicating that the automated method can be applied to large-scale screens.

[Place **Figures 4** and **Figure 5** here]

To evaluate the reproducibility of results among different experimenters, images from a plate containing 6 wells of worms that were fed either *Pseudomonas aeruginosa* MPAO1 or *Escherichia coli* OP50, were acquired by three individuals, two of whom had no prior experience imaging worms using these protocols. Images collected from each well contained anywhere between 30–115 detected worms. A non-significant difference in aggregation was detected in worms from the same wells that were imaged by the three experimenters. While the average number of aggregates per intestine remained very consistent between the three experimenters for worms fed MPAO1 and OP50, there were some statistically significant differences in the average number of aggregates but only in worms colonized by MPAO1 (**Supplemental Figure 2**). These results highlight the reproducibility of the results even between inexperienced experimenters.

To ensure that the reproducibility of aggregate quantification is not significantly influenced by worm position, a set of 15 worms was selected and imaged 15 separate times following agitation in between each image capture using a pipette tip. Images of aggregates in worms fed with *E. coli* OP50 and *P. aeruginosa* MPAO1 were collected and analyzed using CellProfiler. The average number of aggregates from each of these different sets of images was slightly but non-significantly different, further supporting the reproducibility of this approach (**Supplemental**

**Figure 3).**

Colonization of the *C. elegans* intestine with gram-negative enteric pathogens has been shown to disrupt proteostasis across tissues, with *P. aeruginosa* being among the most potent inducers of polyQ aggregation<sup>9</sup>. To determine whether these optimized protocols will successfully detect and quantify *P. aeruginosa*-mediated enhancement of aggregation, worms expressing intestinal polyQ were colonized with *E. coli* OP50 (control bacteria), and *P. aeruginosa* MPAO1, sections 1–8 were conducted. The acquired images were analyzed using CellProfiler (section 9, **Supplemental File 1**). The results of automated quantification show a significant increase in the number of aggregates induced by *P. aeruginosa* MPAO1, consistently resulting in a two-fold enhancement compared to worms fed with control *E. coli* OP50 (**Figure 6**).

[Place **Figure 6** here]

The optimized pipeline was designed to support large-scale screens for conditions that affect proteostasis. To test the feasibility of this approach in screening large libraries of bacteria for their effect on host proteostasis, the pipeline described herein was employed (sections 1–9) to test the effect of 90 *P. aeruginosa* non-essential gene knock-out mutant strains on polyQ aggregation<sup>18</sup>. This pilot screen is part of a larger project designed to screen all *P. aeruginosa* non-essential mutant strains for their ability to influence host proteostasis. Out of 90 bacterial strains tested, colonization of *C. elegans* intestine with one candidate showed a significant decrease in the number of aggregates (**Figure 7**). Follow-up experiments to evaluate the sensitivity of this assay were performed via manual aggregate counts from a random selection of 6 *P. aeruginosa* mutants that differed non-significantly from the MPAO1 control. These experiments were performed using the more traditional 6 cm NGM plates, transferring worms onto test strains as L1's to recapitulate previously established methods<sup>9</sup>. The confirmation experiments by manual counting revealed that none of the mutants, including the one that significantly decreased the number of aggregates (**Figure 7**), affected polyQ aggregation (**Supplemental Figure 4**). In addition, the subtle changes in aggregation observed in the screen of the 90 mutant strains were not detected among manual counts of selected candidates, indicating that such changes could arise because of biological and experimental variability, such as low n value. Collectively, the results indicate that while our method can reliably pick up significant changes, subtle ones will likely be missed, and all potential candidates will have to be individually confirmed.

[Place **Figure 7** here]

To manage the large amount of data generated by CellProfiler, a Graphical User Interface (GUI) was developed to automate data processing and organization (**Figure 8**). The GUI was developed using Tkinter, an open-source Python cross-platform widget toolkit. From the given metadata, the application extracts the number of aggregates (column K) from each well (Column J) present in a plate. A Python data handling library called “Pandas” was used to carry out the aforementioned process. The GUI application provides drag-and-drop support for users to upload data files. The data in each file are stored in the form of a two-dimensional tabular structure

called a data frame. An empty dictionary pair is initialized for every unique well found within the data frame. Next, the distinct aggregates found in each well are counted and appended to their respective dictionary pairs. The column with lesser data is padded with empty valued strings to ensure that each column is even in size. Finally, the structure is converted to a data frame which is exported in the form of a spreadsheet into the directory specified by the user.

[Place **Figure 8** here]

#### **FIGURE AND TABLE LEGENDS:**

**Figure 1: Workflow visual representation.** The major steps of the protocol include five distinct stages: worm preparation and age-synchronization (steps 1–5), intestinal colonization/worm treatment (step 6), sample preparation for imaging (step 7), image acquisition (step 8), and image processing (step 9). The “Sections” of the protocol are referenced as “Steps” in the figure.

**Figure 2: The use of FUDR improves image quality by reducing progeny.** FUDR-supplemented plates eliminate *C. elegans* progeny compared to worms grown on non-FUDR control NGM plates seeded with *E. coli* OP50. Images were acquired at 25.2x magnification (40x magnification with a 0.63x camera adapter). Scale bars = 500  $\mu$ m.

**Figure 3: Freezing improves aggregate detection.** (A) Fluorescent images of *C. elegans* expressing intestinal polyQ44::YFP before and after freezing. Inserts represent close-up images of the selected area. Scale bars = 500  $\mu$ m. (B) Average number of aggregates per intestine in worms colonized with *P. aeruginosa* MPAO1 before and after freezing using manual or automated (pipeline) aggregate quantification. Data represent two biological replicates (n = 60–109). Statistical significance was calculated using Student’s t-test (\*\*\*\* p < 0.0001). Error bars represent the standard error of the mean (SEM).

**Figure 4: Aggregate detection using CellProfiler.** (A) Brightfield image used to identify worm bodies. (B) Original fluorescent image acquired using GFP channel and used to identify and quantify a total number of intestinal polyQ44::YFP aggregates. (C) Aggregates identified using CellProfiler. (D) A total number of identified aggregates superimposed over the original fluorescent image with worm and aggregate outlines. Image capture and processing were performed using the settings described in sections 8–9. Panels E–H represent close-up images of the corresponding outlined regions in images A–D. Images were acquired at 25.2x magnification (40x magnification with a 0.63x camera adapter). Scale bars = 500  $\mu$ m.

**Figure 5: Efficacy of automated aggregate quantification.** (A) Average aggregate number per intestine in worms colonized with control *E. coli* OP50 using manual counting (Manual) and automated CellProfiler-based quantification (Pipeline). Results represent data analyzed in three separate trials (T1–T3) (n = 90–571). (B) The average number of aggregates per intestine was obtained using manual or automated (Pipeline) aggregate quantification. Statistical significance was calculated using Student’s t-test (\* p < 0.05, \*\* p < 0.01). Error bars represent SEM.

**Figure 6: The average number of aggregates per intestine in worms colonized with control *E.***

***coli* OP50 and *P. aeruginosa* MPAO1.** The number of aggregates per intestine was assessed using CellProfiler (sections 8–9). Data are represented as the average number of aggregates per intestine in worms colonized with OP50 (n = 1068) and MPAO1 (n = 1557). Statistical significance was calculated using Student's t-test (\*\*\*\* p < 0.0001). Error bars represent SEM.

**Figure 7: The number of aggregates per intestine in a representative sample set of worms colonized by 92 bacterial strains.** Data are represented as the average number of aggregates per intestine normalized to that of worms colonized with MPAO1. Dotted lines represent the average number of aggregates in worms colonized with MPAO1 (top, open circle) and OP50 control (bottom, open square). Solid symbols represent 90 distinct knock-out mutant strains of *P. aeruginosa* MPAO1. The average number of aggregates per worm between worms colonized with MPAO1 and a single mutant was statistically significant. Gray circles represent samples that were confirmed manually (**Supplemental Figure 4**). Statistical significance was calculated using one-way analysis of variance (ANOVA) followed by multiple comparison Dunnett's post-hoc test (\*\* p < 0.01, \*\*\*\* p < 0.0001). Error bars represent SEM.

**Figure 8: Graphical User Interface.**

**Supplemental Figure 1: Detection of muscle-specific polyQ aggregates.** Worms expressing muscle-specific polyQ35::YFP were plated as L1s and cultured on OP50 for 48 h. Once worms developed into young adults, they were transferred to 24-well NGM plates, supplemented with 100 µg/mL FUDR and seeded with MPAO1 for an additional 72 h before imaging. (A) Brightfield image used to identify worm bodies. (B) Original fluorescent image acquired using GFP channel. (C) Aggregates identified using CellProfiler. (D) A total number of identified aggregates superimposed over the original fluorescent image with worm and aggregate outlines. Image capture and processing were performed using the settings described in sections 8–9. Panels E–H represent close-up images of the corresponding outlined regions in images A–D. Scale bars = 500 µm.

**Supplemental Figure 2: Reproducibility of aggregate quantification between different experimenters.** Average number of aggregates quantified using CellProfiler for 6 wells of worms colonized with *P. aeruginosa* MPAO1 (black bars) and 6 wells of worms colonized with control *E. coli* OP50 (gray bars). Each well was imaged by three experimenters (AVS, DMC, RDH). Data are represented as the average number of aggregates per intestine (n = 30–115). Statistical significance was calculated using one-way ANOVA followed by Tukey's multiple comparisons test (\* p < 0.05, \*\* p < 0.01). Error bars represent SEM.

**Supplemental Figure 3: The effect of worm position on the reproducibility of aggregate quantification.** Average aggregate number per intestine in worms colonized with control *E. coli* OP50 (gray bars) and *P. aeruginosa* MPAO1 (black bars). Results represent the average number of aggregates per intestine (n = 15) quantified using CellProfiler. The position of worms within the wells was changed by agitation in between each acquisition. No statistically significant differences were found in either group. Statistical significance was calculated using one-way ANOVA followed by Tukey's multiple comparisons test. Error bars represent SEM.

**Supplemental Figure 4: Confirmation of the pilot screen with manual counting.** The average number of aggregates per intestine was quantified manually. Data represent aggregation profiles of worms colonized with six MPAO1 knock-out mutants (gray circles **Figure 7**) compared against wild-type MPAO1 and OP50 controls (n = 30). Statistical significance was calculated using one-way ANOVA followed by multiple comparison Dunnett's post-hoc test (\*\*\*\* p < 0.0001). Error bars represent SEM.

**Supplemental Figure 5: The effect of FUDR on intestinal polyQ aggregation.** Data are represented as the average number of polyQ44::YFP aggregates per intestine (n = 20). Worms were transferred onto control (no FUDR) or FUDR-containing plates (100 µg/mL) after 48 h of growth at 25 °C on *E. coli* OP50. Manual counts were collected after an additional 48 h. Statistical significance was calculated using Student's t-test (ns = not significant). Error bars represent SEM.

**Supplemental File 1: Proteostasis pipeline.** Downloadable image analysis pipeline for use in CellProfiler. Instructions for application can be found in section 9.

**Supplemental File 2: Training set untangling worm.** File to be uploaded into the "UntangleWorms" module. This particular training set is specific to the worms used in the initial approach. Alterations in worm size and shape will change the accuracy and quality of identification. It may be necessary to create a more personalized training file. Instructions for creating a new training set can be found at the official CellProfiler website<sup>17</sup>.

**Supplemental File 3: Graphical User Interface for Windows Operating System.** gui\_windowsOS\_64x.zip.

**Supplemental File 4: Graphical User Interface for Mac Operating System.** gui\_MacOS\_64x.zip.

## DISCUSSION:

The described protocol outlines procedures for *C. elegans* culturing, imaging, and image processing that incorporates CellProfiler, an open-source image analysis software. The representative results demonstrate reproducibility, reduction of bias, and scalability. This standardized procedure will improve screening strategies employed with large bacterial, genomic, or drug libraries. While other automated *C. elegans* methods of object detection exists, the described technique offers a standardized, higher-throughput pipeline that integrates culturing, image acquisition, and analysis.

Several variations of worm cultivation had to be tested to optimize the protocol described herein. Initially, worms were transferred to sample bacteria immediately post age-synchronization (L1 stage). However, such an approach resulted in a population of worms with variable sizes, even among worms within the same well. *C. elegans* are known for pathogen avoidance<sup>19</sup>, which could have contributed to the observed variability in size and ultimately affect downstream imaging—worm detection, in particular. To eliminate such variability, the entire NGM area in each well was covered with test bacteria. Furthermore, worms were fed *E. coli* OP50 and allowed to fully

develop into young adults for 48 h at 25 °C. Allowing worms to reach adulthood on *E. coli* OP50 prior to transferring them onto test bacteria resulted in more consistent body size. Additionally, overcrowding and rapid food depletion by progeny were eliminated by supplementing NGM agar with FUDR. The implementation of FUDR removed progeny and enhanced automated worm identification, which was obscured by progeny mixing in with the parental population. However, it is important to be cautious and use appropriate controls when utilizing FUDR, as the compound is known to affect *C. elegans* proteostasis and lifespan<sup>20,21</sup>. Under the conditions described in this protocol, FUDR did not affect intestinal polyQ aggregation (**Supplemental Figure 5**); therefore, its utilization was suitable and beneficial to the described method.

Freezing samples prior to imaging turned out to be a critical step in the successful employment of the pipeline. The aggregate counts prior to freezing were significantly higher than manual counts (**Figure 3B**). Keeping worms at -20 °C for 18–48 h prior to imaging reduced background fluorescence and ultimately improved aggregate detection (**Figure 3A**). The effects of freezing on aggregate detection have only been investigated for polyQ and should not be generalized to other models without further investigation of such effects.

Despite all the conditions being kept the same, it was observed that the average number of aggregates per worm could vary between different runs, while the ratio between the number of aggregates in animals colonized with OP50 versus MPAO1 remained consistent (**Figure 6, Supplemental Figure 2, Supplemental Figure 5**). Therefore, it is essential to always include *E. coli* OP50 control, or any additional suitable reference controls, in every run. Such variability in aggregate counts between experiments could be influenced by environmental conditions (temperature, humidity)<sup>22,23</sup> or genetic background<sup>8</sup>. In fact, it was observed that after prolonged culture, intestinal fluorescence drastically decreased or was completely lost, which required thawing a new strain from frozen stock. The observed decrease in fluorescence could be a result of genetic changes that suppress toxic transgenes, such as those expressing polyQ. Nonetheless, the exceptional reproducibility of the results observed between different experimenters (**Supplemental Figure 2**), between biological replicates (**Figure 5**), and within the same sample (**Supplemental Figure 3**) emphasize on the strength of this approach.

Numerous reports have employed intestinal polyQ to study proteostasis<sup>9,11–13,24,25</sup>. However, a direct comparison between results cannot be made due to variability between experimental approaches and readout methods. Nonetheless, a few results from previously published data are recapitulated by the automated quantification described herein, including bacterial induction of aggregation<sup>9,13</sup> and a comparable number of aggregates<sup>11</sup>. Collectively, the described pipeline offers a valuable tool to study proteostasis.

The method described herein has some inherent challenges. For example, it requires sufficient time to master all components of this protocol, which is especially true for section 8 of the protocol, which requires familiarity with the assay to determine if the images acquired are appropriate for pipeline analysis. Deviations from the image acquisition settings used in this protocol are possible; however, modification of the settings and worm training set will likely be required. This pipeline can distinguish aggregates of various sizes and those that are touching,

which limits the “blending” of aggregates and ultimately increases the detection sensitivity. However, issues may arise when attempting to identify large aggregates that exceed the accepted size range, as expanding the upper size threshold may lead to errors caused by poor identification, such as the inability to differentiate aggregates that are touching. A balance between accuracy, size, and intensity must be found prior to image analysis. The efficiency of aggregate identification could be further improved by incorporating machine learning to create a neural network capable of enhancing aggregate detection. Such improvements are currently being explored and will greatly assist in addressing current issues such as the detection of aggregates that lie on different focal planes or that have abnormal shapes.

One notable weakness of the described method is the variability in automated aggregate counts, as they are not always recapitulated by manual counts in worms fed different bacterial strains. For example, based on automated counts, worms fed *P. aeruginosa* mutant 53 (M53) had significantly fewer aggregates compared to the wild-type strain (MPAO1) (**Figure 7**); however, confirmation of the hit showed no significant difference (**Supplemental Figure 4**). In general, high-throughput drug screens have a high rate of false-positive hit detection, and the described method is no exception<sup>26</sup>. Thus, it is a critical part of the protocol to confirm all potential hits.

While this protocol was optimized to fit a screening strategy to identify bacteria that affect host proteostasis, each step can be further modified to test the effect of genomic RNAi libraries, small molecules, or other conditions. Additional modifications can be made at each step to suit the requirements of a specific screening strategy. Furthermore, this technique provides a level of flexibility that allows for the optimization of each step to suit a specific model. For example, this approach can be extended to polyQ aggregation in other tissues or extracting other features detected in images such as monitoring gene expression using inducible fluorescent reporters (e.g., heat shock genes), assessing subcellular localization of proteins (e.g., nuclear localization of DAF-16), studying aggregation in other disease models (A $\beta$ <sub>1-42</sub>,  $\alpha$ -synuclein, TDP-43, etc.) or assessing physiological phenotypes, such as worm size.

#### ACKNOWLEDGMENTS:

This work was supported by the National Institutes of Health (1R03AG069056-01) and the Infectious Diseases Society of America funding to DMC. The funders had no role in study design, data collection and analysis, decision to publish, or preparation of the manuscript. We thank the members of the Czyz Lab for proofreading the manuscript. Cartoon figures were generated using BioRender paid license.

#### DISCLOSURES:

The authors have declared that no conflicts of interest exist.

#### REFERENCES:

1. Soto, C. Unfolding the role of protein misfolding in neurodegenerative diseases. *Nature Reviews Neuroscience*. **4** (1), 49–60 (2003).
2. Fang, P., Kazmi, S. A., Jameson, K. G., Hsiao, E. Y. The microbiome as a modifier of neurodegenerative disease risk. *Cell Host & Microbe*. **28** (2), 201–222 (2020).

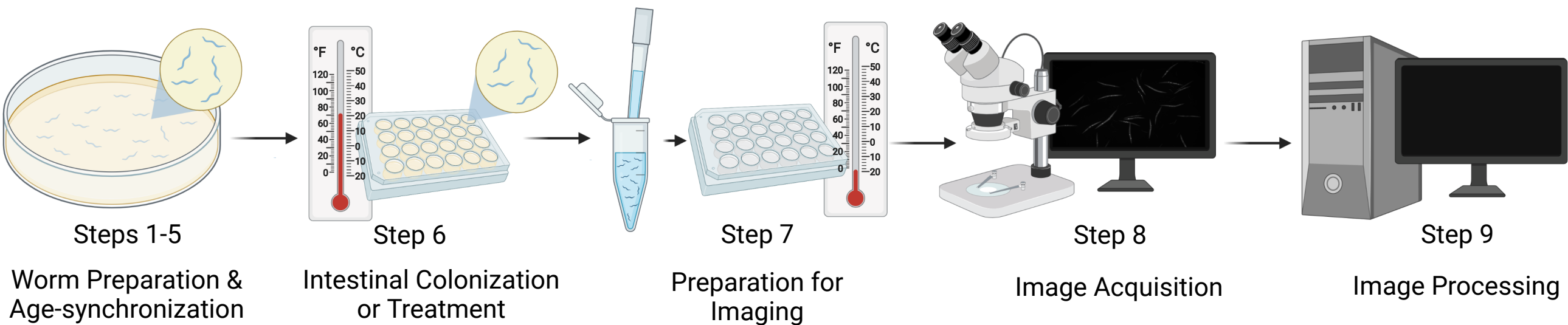


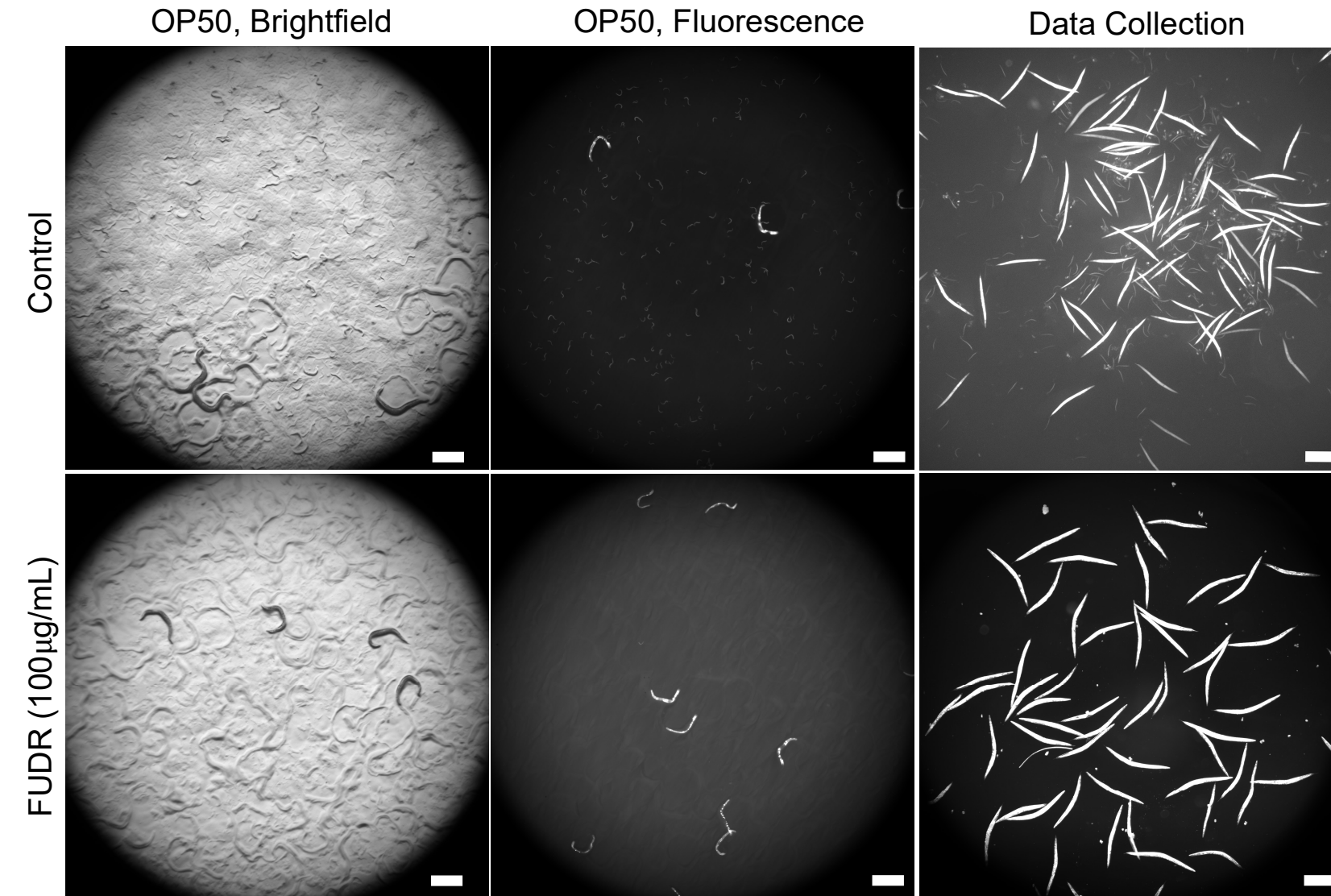
3. Kundu, P., Blacher, E., Elinav, E., Pettersson, S. Our gut microbiome: The evolving inner self. *Cell*. **171** (7), 1481–1493 (2017).
4. Sherwin, E., Dinan, T. G., Cryan, J. F. Recent developments in understanding the role of the gut microbiota in brain health and disease. *Annals of the New York Academy of Sciences*. **1420** (1), 5–25 (2018).
5. Mondal, S. et al. Large-scale microfluidics providing high-resolution and high-throughput screening of *Caenorhabditis elegans* poly-glutamine aggregation model. *Nature Communications*. **7** (1), 13023 (2016).
6. Guisbert, E., Czyz, D. M., Richter, K., McMullen, P. D., Morimoto, R. I. Identification of a tissue-selective heat shock response regulatory network. *PLoS Genetics*. **9** (4), e1003466 (2013).
7. Silva, M. C. et al. A genetic screening strategy identifies novel regulators of the proteostasis network. *PLoS Genetics*. **7** (12), e1002438–e1002438 (2011).
8. Nollen, E. A. et al. Genome-wide RNA interference screen identifies previously undescribed regulators of polyglutamine aggregation. *Proceedings of the National Academy of Sciences of the United States of America*. **101** (17), 6403–6408 (2004).
9. Walker, A. C. et al. Colonization of the *Caenorhabditis elegans* gut with human enteric bacterial pathogens leads to proteostasis disruption that is rescued by butyrate. *PLOS Pathogens*. **17** (5), e1009510 (2021).
10. Goya, M. E. et al. Probiotic *Bacillus subtilis* protects against  $\alpha$ -Synuclein aggregation in *C. elegans*. *Cell Reports*. **30** (2), 367–380.e367 (2020).
11. Kumsta, C., Chang, J. T., Schmalz, J., Hansen, M. Hormetic heat stress and HSF-1 induce autophagy to improve survival and proteostasis in *C. elegans*. *Nature Communications*. **8** 14337 (2017).
12. Prahlad, V., Morimoto, R. I. Neuronal circuitry regulates the response of *Caenorhabditis elegans* to misfolded proteins. *Proceedings of the National Academy of Sciences of the United States of America*. **108** (34), 14204–14209 (2011).
13. Mohri-Shiomi, A., Garsin, D. A. Insulin signaling and the heat shock response modulate protein homeostasis in the *Caenorhabditis elegans* intestine during infection. *Journal of Biological Chemistry*. **283** (1), 194–201 (2008).
14. Hakim, A. et al. WorMachine: machine learning-based phenotypic analysis tool for worms. *BMC Biology*. **16** (1), 8 (2018).
15. Wählby, C. et al. An image analysis toolbox for high-throughput *C. elegans* assays. *Nature Methods*. **9** (7), 714–716 (2012).
16. Jones, T. R. et al. CellProfiler Analyst: data exploration and analysis software for complex image-based screens. *BMC Bioinformatics*. **9** (1), 482 (2008).
17. CellProfiler: an open-source image analysis software at <cellprofiler.org> (2021)
18. Held, K., Ramage, E., Jacobs, M., Gallagher, L., Manoil, C. Sequence-verified two-allele transposon mutant library for *Pseudomonas aeruginosa* PAO1. *Journal of Bacteriology*. **194** (23), 6387–6389 (2012).
19. Schulenburg, H., Ewbank, J. J. The genetics of pathogen avoidance in *Caenorhabditis elegans*. *Molecular Microbiology*. **66** (3), 563–570 (2007).
20. Feldman, N., Kosolapov, L., Ben-Zvi, A. Fluorodeoxyuridine improves *Caenorhabditis elegans* proteostasis independent of reproduction onset. *PLoS One*. **9** (1), e85964 (2014).
21. Van Raamsdonk, J. M., Hekimi, S. FUDR causes a twofold increase in the lifespan of the

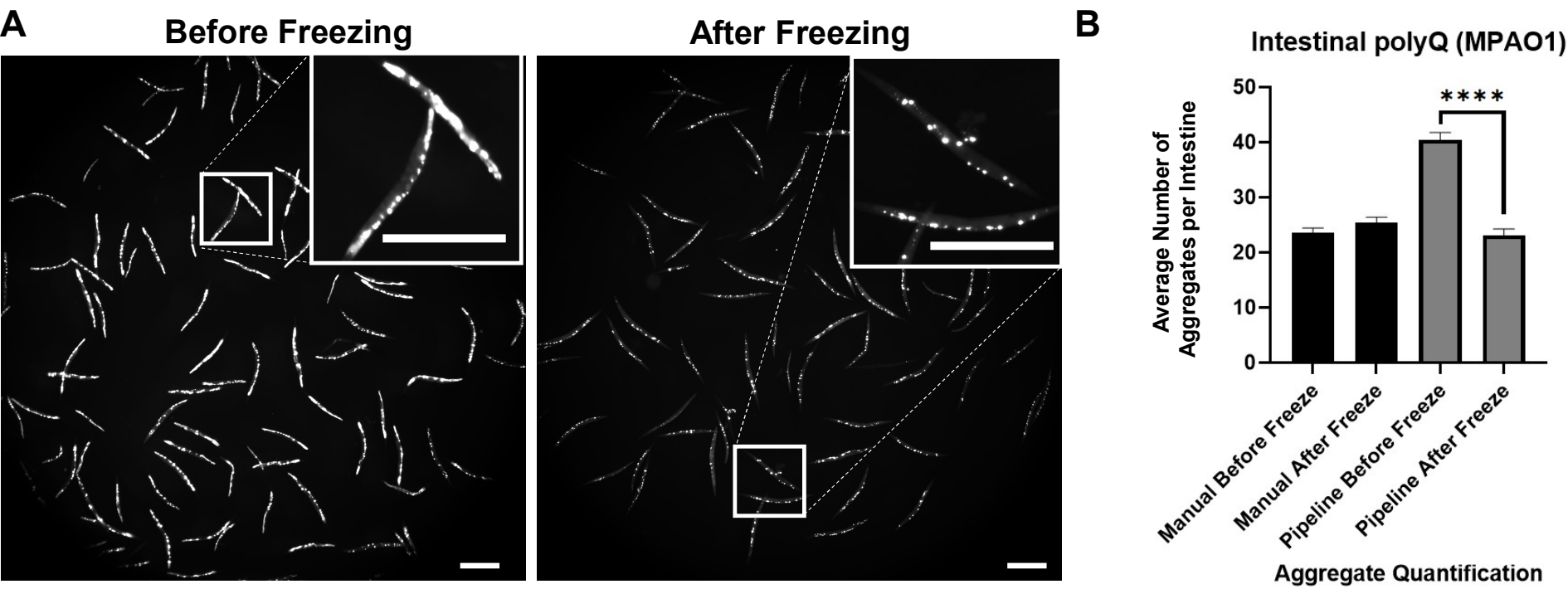
- mitochondrial mutant gas-1. *Mechanisms of Ageing and Development*. **132** (10), 519–521 (2011).
22. Haldimann, P., Muriset, M., Vigh, L., Goloubinoff, P. The novel hydroxylamine derivative ng-094 suppresses polyglutamine protein toxicity in *Caenorhabditis elegans*. *Journal of Biological Chemistry*. **286** (21), 18784–18794 (2011).
23. Shinn-Thomas, J. H. et al. Wrapping culture plates with Parafilm M® increases *Caenorhabditis elegans* growth. *BMC Research Notes*. **12** (1), 818 (2019).
24. Alexander-Floyd, J. et al. Unexpected cell type-dependent effects of autophagy on polyglutamine aggregation revealed by natural genetic variation in *C. elegans*. *BMC Biology*. **18** (1), 18 (2020).
25. Moronetti Mazzeo, L. E., Dersh, D., Boccitto, M., Kalb, R. G., Lamitina, T. Stress and aging induce distinct polyQ protein aggregation states. *Proceedings of the National Academy of Sciences of the United States of America*. **109** (26), 10587–10592 (2012).
26. Sink, R., Gobec, S., Pecar, S., Zega, A. False positives in the early stages of drug discovery. *Current Medicinal Chemistry*. **17** (34), 4231–4255 (2010).

Figure 1

[Click here to access/download;Figure;Fig1.pdf](#)







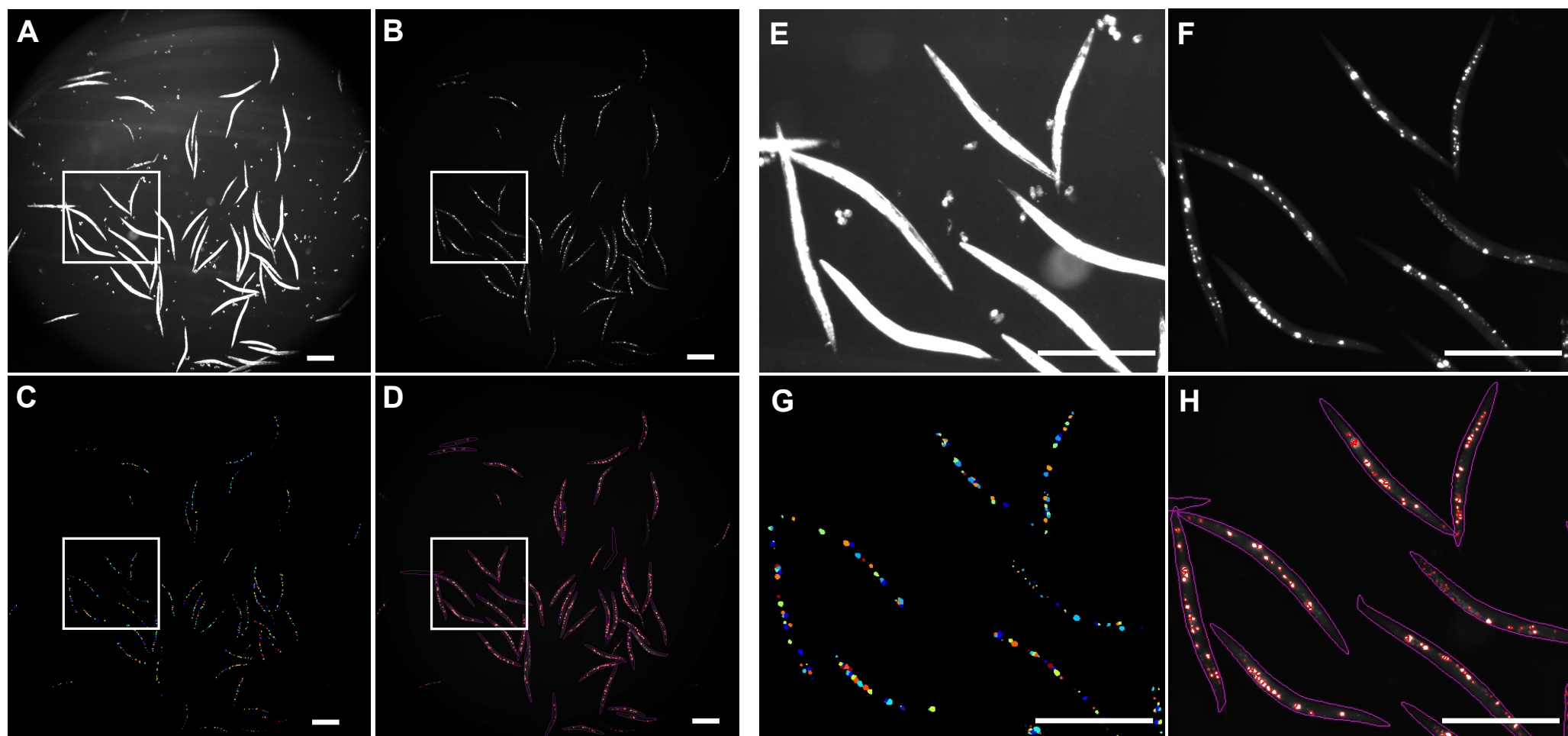


Figure 5

[Click here to access/download;Figure;Fig5.pdf](#)

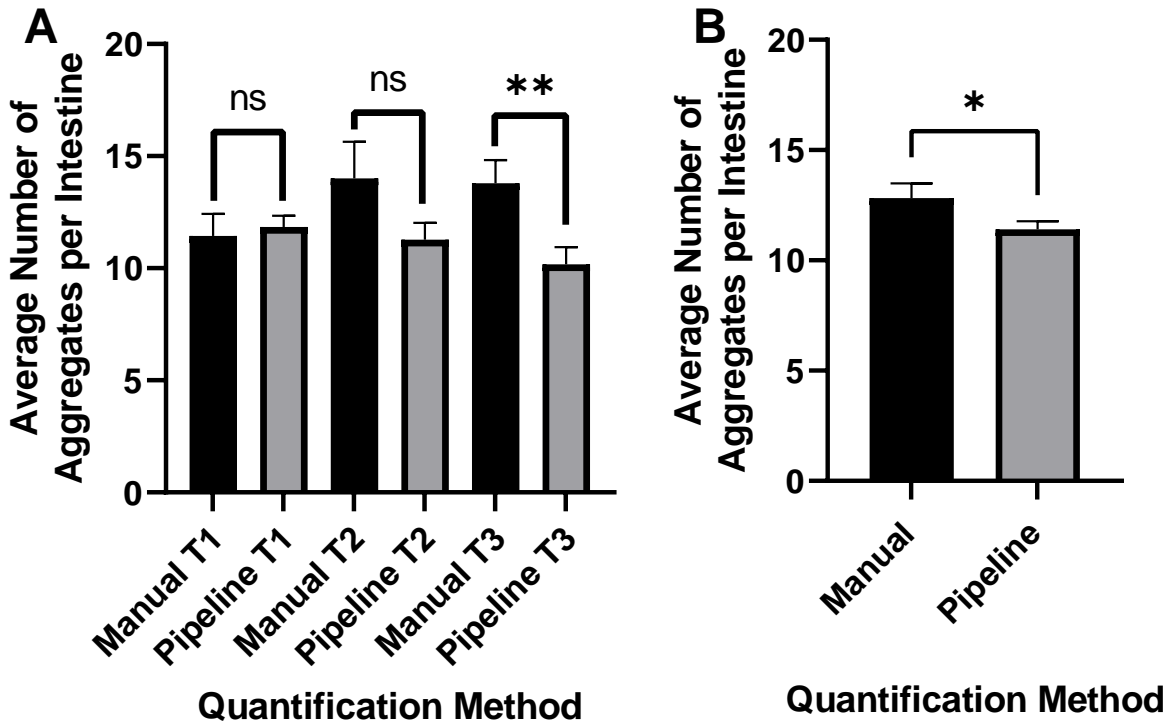


Figure 6

[Click here to  
access/download](#) 

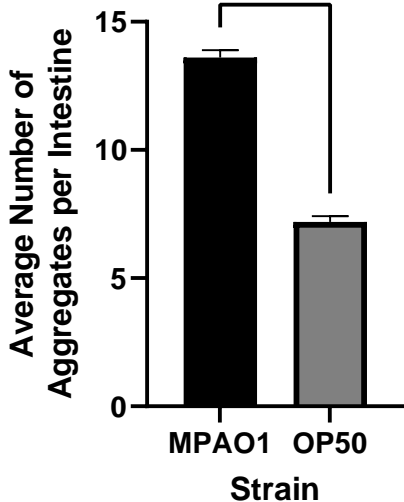
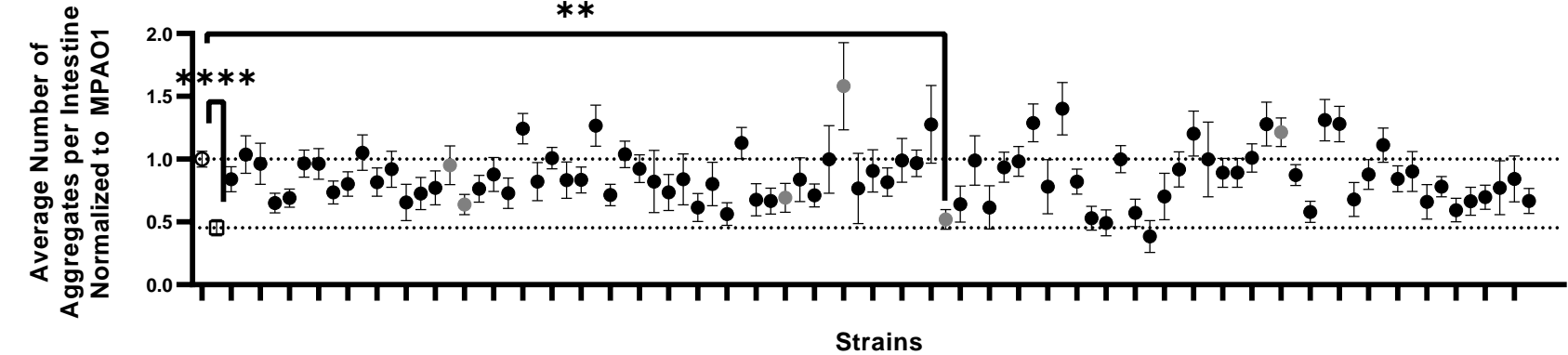
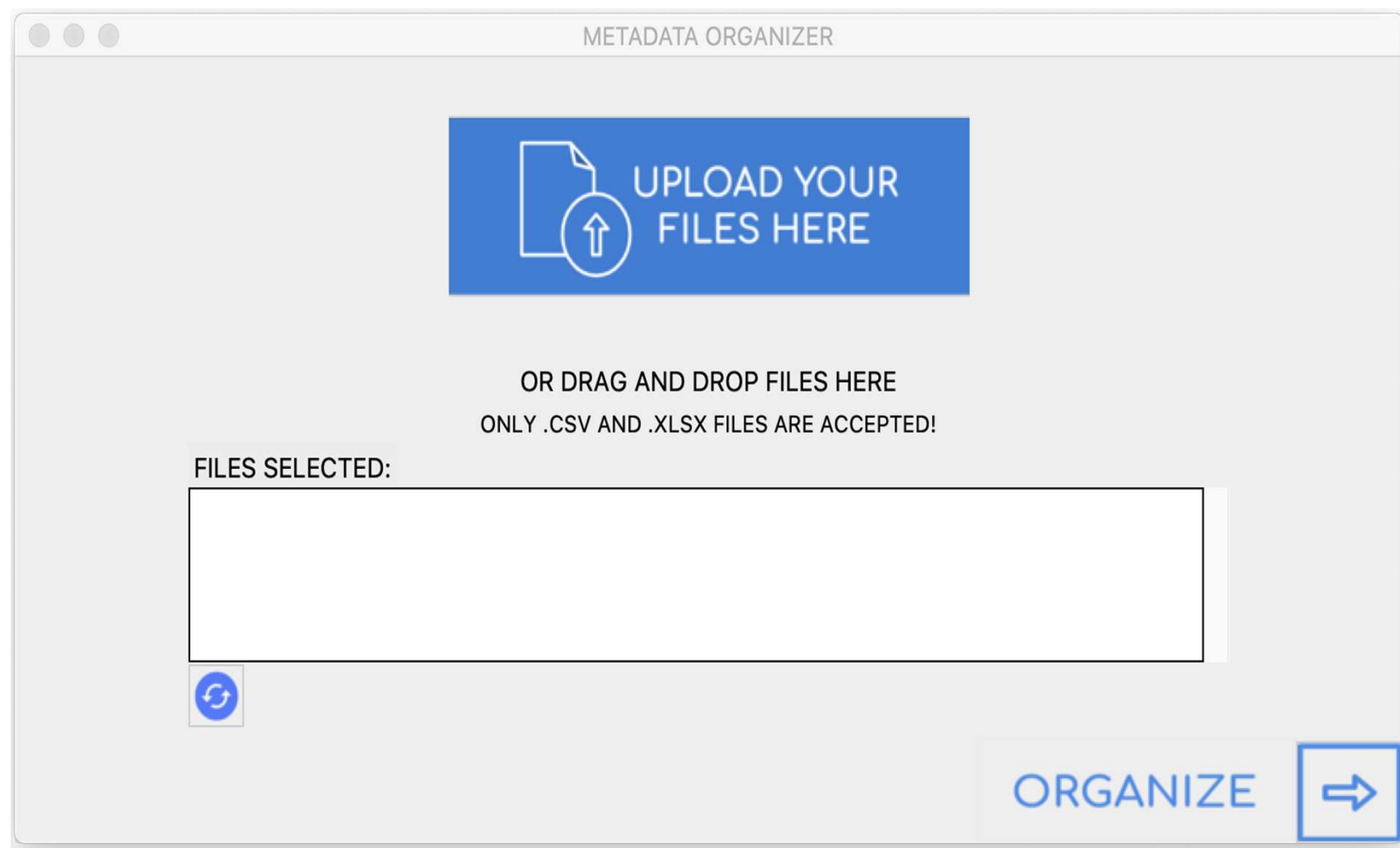




Figure 7

[Click here to access/download;Figure;Fig7.pdf](#) 



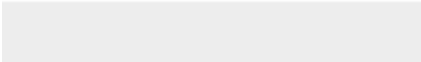




[Click here to access/download](#)

**Table of Materials**

**[Materials\\_Reagents\\_Table-62997R1.xlsx](#)**





College of Agricultural and Life Sciences  
Department of Microbiology and Cell Science

Daniel M Czyż, Ph.D.  
Assistant Professor  
PO Box 110700  
Microbiology Bldg. 981, Rm. 1004  
Gainesville, FL 32611-0700  
Office: 352-392-0237  
Lab 352-846-0965

August 23, 2021

*JoVE*

Dear Dr. Krishnan –

Please find attached a revised version of manuscript # JoVE62997 entitled “Automating Aggregate Quantification in *Caenorhabditis elegans*.” We would like to thank you for the opportunity and allowed time to revise our manuscript. We include a point-by-point response to each reviewer's comments and have updated the manuscript accordingly with the recommendations offered by you and the reviewers.

The revised version of the manuscript includes several of the experimental recommendations suggested by the reviewers. We have included new data that demonstrate technique optimization and reproducibility. In particular, we showed the effect of sample freezing on aggregate enumeration (new Figure 3). We have developed a Graphical User Interface (new Figure 8) software (for Mac and Windows OS) that allows us to automate the processing of large excel datasets generated using CellProfiler. While we did not feel it was appropriate to expand our approach using additional models because of the extensive optimization that would expand the manuscript, we did demonstrate its feasibility to detect muscle-specific polyQ (new Supplemental Figure 1). Furthermore, we demonstrated reproducibility between individual experimenters by having three separate individuals collect data from the same samples (new Supplemental Figure 2) . We also acquired images and analyzed data from the same worms positioned in 15 different orientations (new Supplemental Figure 3). Additional controls, such as the effect of FUDR on aggregation, were also added (new Supplemental Figure 5).

As a result of these additional experiments, we have added two additional authors to the manuscript: Carol Navya Pagolu and Samantha M. Enslow, who contributed to revision experiments. All authors agreed to and acknowledged the addition.

As stated in our initial submission, we believe our study will be of interest to those who employ *C. elegans* as a model to study the effect of bacteria on proteostasis and those investigating other factors, conditions, and small molecules. Please see the attached document titled “Reviwe\_Response,” which addresses each issue raised by the reviewers. Thank you very much for handling the review process and for providing guidance on how to make our study suitable for publication in JoVE. We very much appreciate the time and attention you have devoted to this submission.

Yours sincerely,

A handwritten signature in black ink, appearing to read 'Daniel Czyż'. The signature is fluid and cursive, with the first name 'Daniel' and the last name 'Czyż' clearly distinguishable.

Daniel M Czyż, Ph.D.

Assistant Professor of Microbiology and Cell Science

## **Review Response**

### Editorial Comments:

Thank you for your comments. There may be some formatting issues with each step that should clear once all changes are approved. Please find our responses below addressing each concern.

1. Please take this opportunity to thoroughly proofread the manuscript to ensure that there are no spelling or grammar issues.

#### **Response:**

We have carefully proofread the manuscript and addressed any spelling or grammar issues

2. Please provide an institutional email address for each author.

#### **Response:**

Email addresses for each author were added to the manuscript (lines 16-21).

3. Please revise the text to avoid the use of any personal pronouns (e.g., "we", "you", "our" etc.).

#### **Response:**

The manuscript was carefully reviewed to eliminate all personal pronouns.

4. JoVE cannot publish manuscripts containing commercial language. This includes trademark symbols (™), registered symbols (®), and company names before an instrument or reagent. Please remove all commercial language from your manuscript and use generic terms instead. All commercial products should be sufficiently referenced in the Table of Materials.

For example: TX-400, Leica, CoolLED pE-300lite, CellProfiler, etc.

#### **Response:**

Commercial Language was removed from the revised manuscript and listed in the reagent table. Reference to CellProfiler open-source software is necessary throughout the paper. CellProfiler is an open-source software and not a commercial product.

5. Please note that your protocol will be used to generate the script for the video and must contain everything that you would like shown in the video. Please add more details to your protocol steps. Please ensure you answer the “how” question, i.e., how is the step performed? Alternatively, add references to published material specifying how to perform the protocol action. Please add more specific details (e.g., button clicks for software actions, numerical values for settings, etc.) to your protocol steps. There should be enough detail in each step to supplement the actions seen in the video so that viewers can easily replicate the protocol.

**Response:**

We added an extra level of details to the video protocol (highlighted region)

6. Line 90 (new 102): Please specify the conditions for autoclaving (temperature, pressure, duration, etc.).

**Response:**

Line 102-103: Autoclave the mixture for 45 minutes at 121°C and a pressure of 21 pound-force per square inch (psi).

7. Line 93-94 (new 108): How long is the solution placed on magnetic stirrer. Any specific temperature and stirring speed?

**Response:**

Line 108-109: Mixing may be performed for 1 min at 700 RPM.

8. Line 95-96 (new 111): Please specify the volume of the media used for making plates.

**Response:**

Line 111-112: Pour approximately 20 mL of the mixture per 10 cm plate. Pour until mixture gradually fills the entire bottom surface. Alternatively, use a graduated serological pipette.

9. Line 114-115 (new 141): Please specify how the overnight culture of E.coli is prepared.

**Response:**

Lines 141:-148:

- 3.1 To prepare an overnight *E. coli* OP50 culture, add a 200  $\mu$ L of a bacterial aliquot from a frozen stock into a 500 mL Erlenmeyer flask containing 250 mL of fresh and sterile Luria broth (LB). The volume of the media depends on the number of plates that need to be seeded. If preparing other bacterial cultures to be tested, inoculate a 16-mL culture tube containing 5 mL of growth medium with bacteria from frozen stock using a sterile micropipette tip.
- 3.2 Incubate overnight in a 37 °C incubator, shaking at 220 RPM.

10. Line 120 (new 154): 1 mL of culture? Is this E coli overnight culture? Is the culture spread on the plate?

**Response:**

Lines 154-155: We have added the following text: Dispense 1-2 mL of the overnight *E. coli* OP50 culture onto the center of each 10 cm NGM plate. This culture does not need to be spread around the NGM plate.

11. Line 141 (new 179): Please specify how the M9 solution is prepared (the constituents of the solution and their respective weights used)

**Response:**

Lines 179-181: Wash gravid hermaphrodites off of 10 cm OP50 plates using filter-sterilized M9 solution (5.8 g  $\text{Na}_2\text{HPO}_4 \bullet 7\text{H}_2\text{O}$ , 3.0 g  $\text{KH}_2\text{PO}_4$ , 5 g NaCl, 0.25 g  $\text{MgSO}_4 \bullet 7\text{H}_2\text{O}$ , in 1 L of dd  $\text{H}_2\text{O}$ )

12. Please include a one-line space between each protocol step and then highlight up to 3 pages of the Protocol (including headings and spacing) that identifies the essential steps of the protocol for the video, i.e., the steps that should be visualized to tell the most cohesive story of the Protocol. Remember that non-highlighted Protocol steps will remain in the manuscript, and therefore will still be available to the reader.

**Response:**

One line spacing has been added in between all steps of the protocol. All sections desired for the video have been highlighted.

13. As we are a methods journal, please ensure that the Discussion explicitly covers the following in detail in 3-6 paragraphs with citations:



- a) Critical steps within the protocol
- b) Any modifications and troubleshooting of the technique
- c) Any limitations of the technique
- d) The significance with respect to existing methods
- e) Any future applications of the technique

**Response:**

We have updated the discussion section to cover the above points.

14. Figure 1: Please label the figure to make it more informative.

**Response:**

Figure 1 has been updated.

15. Figure 2/3: Please include scalebars in all the images of the panel. Please provide the details of magnification used in the Figure Legends.

**Response:**

Scale bars have been added to all images, and the magnification details were added to figure legends.

16. Please ensure that the Table of Materials include all the essential chemicals, reagents and equipment used in this study. Please sort the table in alphabetical order.

**Response:**

The table has been updated and alphabetized.

## Reviewer 1:

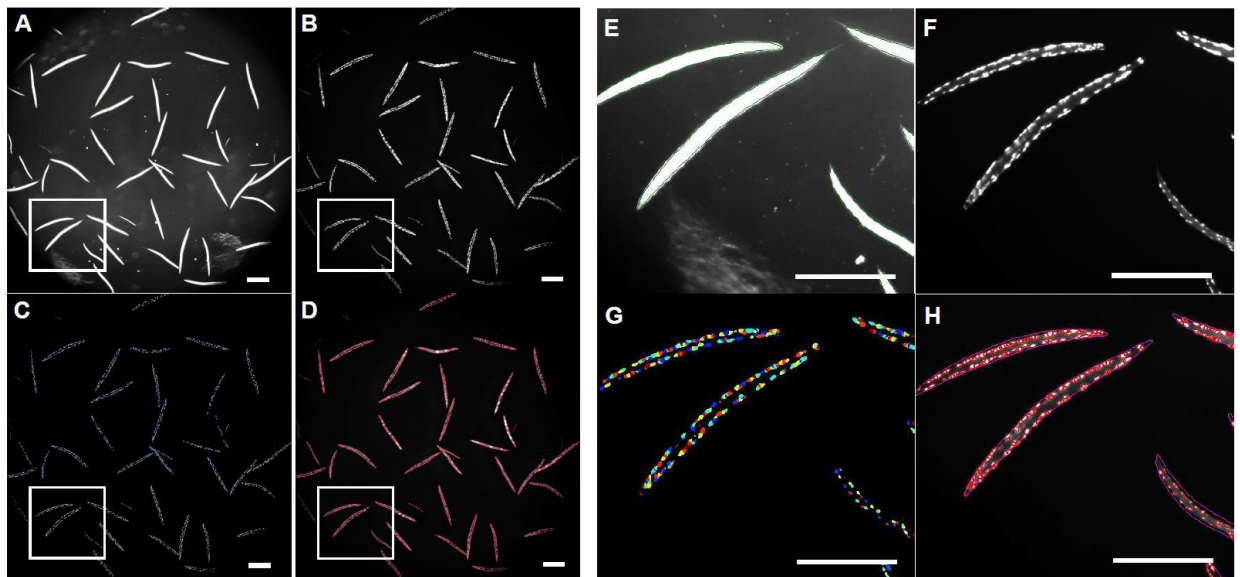
### Major Concerns:

1. It would be helpful to the scientific community to know if the method and workflow described herein can be used to quantify protein aggregates in other tissues such as muscle and neurons. Since polyQ proteins have already been stably expressed in these tissues with YFP tags, it seems that testing this would be fairly straightforward and would make the method more broadly applicable.

## Response:

We thank the reviewer for bringing up other tissue-specific polyQ models. We agree that our approach could be used to quantify polyQ aggregates in the muscle. In fact, we acquired images and ran that analysis using CellProfiler. We were able to successfully detect aggregates (Supplemental Figure 1); however, processing images of muscle polyQ will require additional optimization to determine the best polyQ length, age of worms, and exposure time. Also, magnification will have to be optimized to maximize the detection of aggregates that are located in a different focal plane. We believe these optimizations would make the submitted manuscript too extensive. We have not explored the application of our approach using neuronal polyQ; however, our approach will most likely be feasible but will require the acquisition of images at higher resolution and magnification, which will affect throughput.

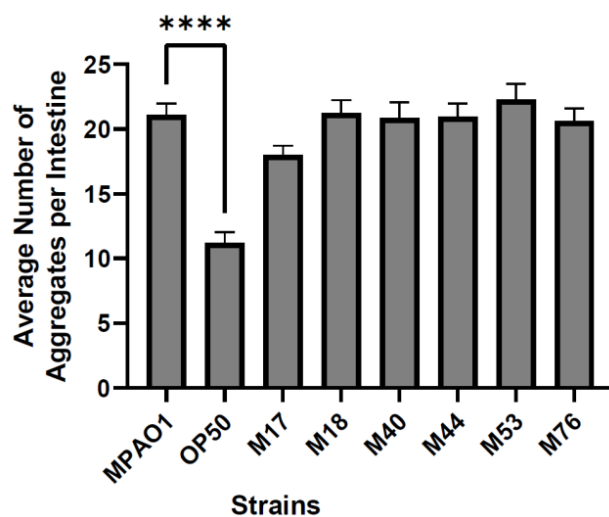
We have updated the text accordingly (lines 456-463) and added Supplemental Figure 1 (lines 637-646, see below) that demonstrates automated detection of muscle-specific polyQ.



2. I'd be interested to know more about the sensitivity of this assay. The authors note that *P. aeruginosa* is one of the strongest inducers of polyQ aggregation, which was recapitulated nicely in their automated analysis. However, it would be nice to know whether the protocol described here can likewise be used to detect more subtle changes in proteostasis. Thus, the authors might consider selecting some of the 90 bacterial strains that showed subtle, not statistically significant, effects in their assay and compare their results to those obtained by manual aggregate counting.

**Response:**

The reviewer brings an important point. To address this concern, we performed manual aggregate quantification in worms colonized by six selected mutants (M17, M18, M40, M44, M53, and M76) that show subtle differences in polyQ aggregation observed in the original screened plate (Figure 7). Among these mutants, M53 was the only one that resulted in significantly fewer polyQ aggregates upon intestinal colonization; however, manual counting (see below) did not confirm that potential candidate. Overall, in agreement with the CellProfiler quantification, we did not detect any significant changes in polyQ aggregation based on manual counts. The subtle changes observed with automated counting were not detected with manual counts. We have added a new figure (Supplemental Figure 4, see below) and text to the manuscript (lines 545-559).

**Minor Concerns:**

1. Section 5.0 "Age synchronization": Indicate whether canonical tubes should be polystyrene or polypropylene (or if it doesn't matter).

**Response:**

We have used polystyrene conical tubes. We have added this information to the manuscript (lines 186-187).

2. My understanding is that the final imaging is done on killed (frozen) animals in 24-well plates that have no agar media, such that the worms are laying directly on the bottom of the well. Please specify whether these are flat or round bottom wells (or if it doesn't matter).

**Response:**

Flat-bottom wells should be used for imaging. We have added this information to lines 297-298.

## Reviewer #2:

Manuscript Summary: Vaziriyani-Sani et al present a useful protocol to quantify the number of fluorescent polyQ aggregates in *C. elegans*. They provide a method for *C. elegans* maintenance, imaging and image analysis. Overall, the procedure is easy to follow and provides an excellent level of detail.

### Major Concerns:

Some more details about image collection settings are needed in Section 8 Imaging. Specifically, the minimum number of pixels required per aggregate/ an appropriate magnification range to use and information relating to intensity of aggregates vs background. Details of an exposure time of 500 ms and 100% intensity are useful for the system specified but an indication of the fluorescence intensity of an aggregate in a typical image would be useful for users of other systems. A threshold intensity for distinguishing aggregates from background is likely to be an important factor in using this method and so some discussion of how this is calculated and when this CellProfile pipeline can be directly applied vs when it will need to be modified is needed. Details of typical background fluorescence values would be useful to apply this more widely.

### Response:

We thank the reviewer for this insightful feedback. We have addressed the raised concerns in lines 313-321 (Note). We acknowledged that different microscope systems might be used and provided more objective methods for acquiring images. We have provided a range for aggregate size (between 1 and 10 pixels) and intensity (between 0.10-1.0) for GFP images as well as common values of background fluorescence (below 0.10) detected across images. We also added a range for worm size (250-350 pixels) and worms (0.70-1.0) and background (0.10-0.20) intensities across brightfield images.

Additional information is provided in lines 330-354: Protocols have been modified to include information on how image acquisition can be standardized to closely replicate images presented in this paper by measuring the intensity and size of objects in the software preview mode. This information can then be used to alter image settings if necessary.

### Minor Concerns:

Sections 1-5 describe standard *C. elegans* maintenance and synchronization methods. However, Figure 2 highlights the importance to the protocol of addition of FUdR. It would be useful if section 2.2 in the protocol was highlighted or a note added here to emphasize the importance of this addition so it is not overlooked.

FUdR is known to impact lifespan as well as fertility and an addition note mentioning the impact of this should be included.

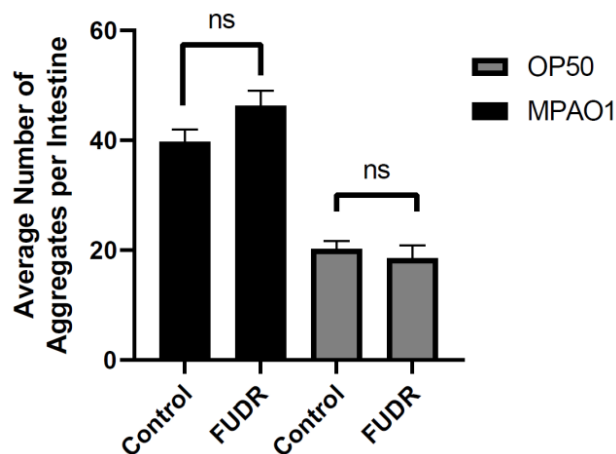
**Response:**

Thank you for this suggestion. We have added a note (lines 125-128) that briefly described the effect of FUDR on reproduction and lifespan.

We have also added Supplemental Figure 5 (see below) and the following text:

-line 230, emphasizing that “It is important to note that these plates must not contain FUDR.”

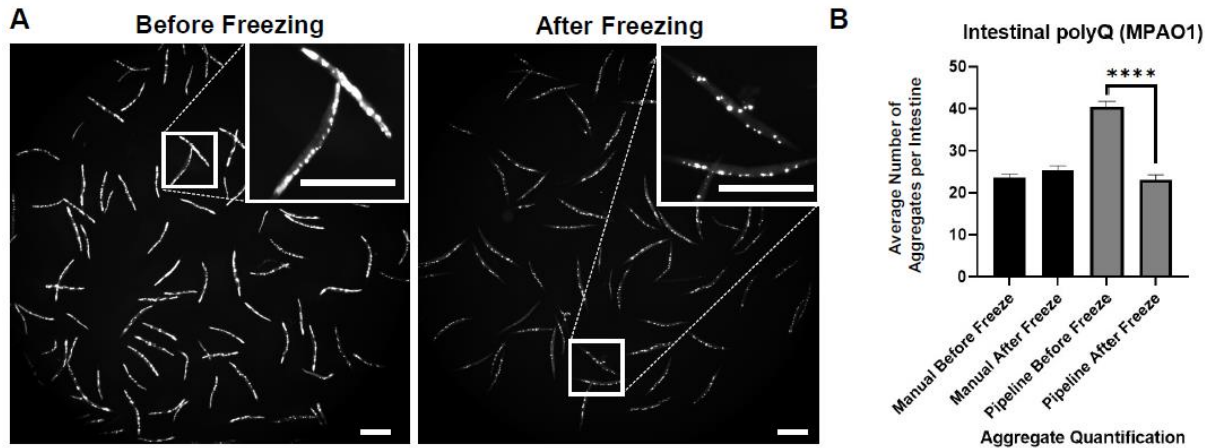
-lines 713-720: Additionally, overcrowding and rapid food depletion by progeny were eliminated by supplementing NGM agar with FUDR. The implementation of FUDR removed progeny and enhanced automated worm identification, which was obscured by progeny mixing in with the parental population. However, it is important to be cautious and use appropriate controls when utilizing FUDR, as the compound is known to affect *C. elegans* proteostasis and lifespan<sup>19,20</sup>. Under the conditions described in this protocol, FUDR did not affect intestinal polyQ aggregation (Supplemental Figure 5, see below); therefore, its utilization was suitable and beneficial to the described method.



Some increased explanation around the freezing protocol in section 7 would be useful. A reference for reduced autofluorescence on freezing would be useful.

**Response:**

The reviewer brings an important point that was not addressed well in the original manuscript. We have performed additional control experiments to demonstrate the rationale of freezing worms (new Figure 3, see below) and added additional explanation to the revised manuscript (lines 475-483). Initially we were freezing worms to prevent further aggregate formation as often the imaging step can take hours if we are handling hundreds of samples simultaneously. We noticed that the freezing step improved aggregate detection. Therefore, the freezing step has a dual purpose that we explained in the revised manuscript in more depth. We have modified the language in lines 274-279 so the purpose of freezing is more clear.



Line 212 (new 275)- "worms must be paralyzed prior to freezing" should I think be changed to "prior to washing" or is levamisole added prior to freezing? This should be clarified.

**Response:**

Thank you for pointing this out. We have changed "freezing" to "washing" (lines 275).

Section 8. A note outlining the image format(s) required could be added.

**Response:**

We have added details on the file format (line 309).

Sections 9.4 -9.7 could made easier to follow for a novice CellProfiler user who may not understand terminology such as module by adding some more details and explicitly stating module names. For example, in 9.6 specifying which module should be selected when selecting the output folder would be useful.

**Response:**

We have added additional and more detailed steps that should make the navigation through CellProfiler more user-friendly (Step 9). Also, Step 9 was selected for video instruction to show novice users how to manipulate the pipeline.

Clarity could also be improved by separating out the steps related to the training set more clearly.

**Response:**

Thank you for pointing this out. Instructions on how to upload the training set have been separated into more steps to facilitate understanding of instructions.

An example set of images is not necessary but would make using the CellProfiler pipeline more user friendly.

**Response:**

We have selected this step to be covered in the training video, which will provide the reader with detailed step-by-step directions on operating CellProfiler.

A product number for the 24 well plates would be useful.

**Response:**

The product number for the 24-well plates used has been included in the materials and reagents table.

**Reviewer 3:**

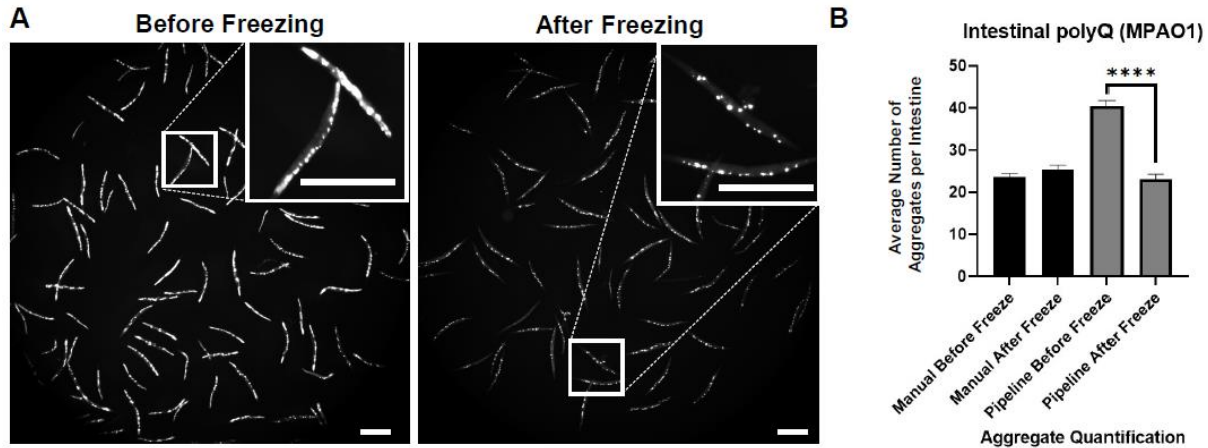
Major Concerns: This methodology is a welcome advancement in the field of proteostasis, since manual aggregate quantification is timeintensive and prone to investigator bias. However, there are several concerns that would need to be addressed prior to publication:

1. The main experimental concern is insufficient validation. The method, including the parts 7.0 (preparing worms for imaging) and 8.0 (imaging), has new techniques and/or procedures introduced, but their effect on aggregation or their ability to accurately represent the number of aggregates that were present before these manipulations is not adequately examined. For example, in 'preparing worms for imaging', how does freezing at -20C affect pre-existing aggregates? Data needs to be shown to compare aggregate numbers with and without freezing, and I would think this should be done using the traditional manual counting, since using the CellProfiler pipeline would mean using not-yet proven method.

**Response:**

We thank the reviewer for bringing this up. We performed control experiments where we compared manual aggregate counts before and after freezing using manual counts and pipeline quantification (new Figure 3, see below). We found no significant difference in aggregate counts before and after freezing when counted manually (Figure 3A). However, CellProfiler detected background fluorescence and counted aggregates as

false positive before freezing (Figure 3B). This problem was eliminated with freezing, and we obtained aggregate counts that are similar to those generated by manual counting. We have updated the revised manuscript lines 475-483 and Lines 713-720.



For the image acquisition and analysis - the authors need to show that their method picks up different types of aggregates, for example, do they accurately capture small vs large aggregates, are they able to separate the closely positioned or 'touching' aggregates, etc. This may require showing images of the aggregates identified by their pipeline side-by-side with high resolution images of the same animal, or comparison of aggregate counts with quantification of SDS-resistant material on gels, since these are polyQs.

#### Response:

We believe Figure 4 already satisfied this concern. Sections of the original images have all been enhanced and show detection of aggregates of all sizes. Additionally, aggregates are in close proximity to each other also seem to be well separated and counted. There is likely some false positive or negative detection but based on our quantification of aggregates in worms colonized by OP50 and PAO1 (manual and automated counts), such false counts are negligible.

Furthermore, it would help for this method to become an accepted one if they were to show that this new method recapitulates published data, for example does it show the same age of aggregation onset, or degree of enhancement/suppression of aggregates as in prior modifier papers?

#### Response:

We thank the reviewer for this suggestion. It is difficult to directly compare our method with what was previously published because of the lack of standardized protocols (hence our protocol). The data that are currently published are generated from polyQ-expressing worms at various temperatures, mutant backgrounds, food sources, and



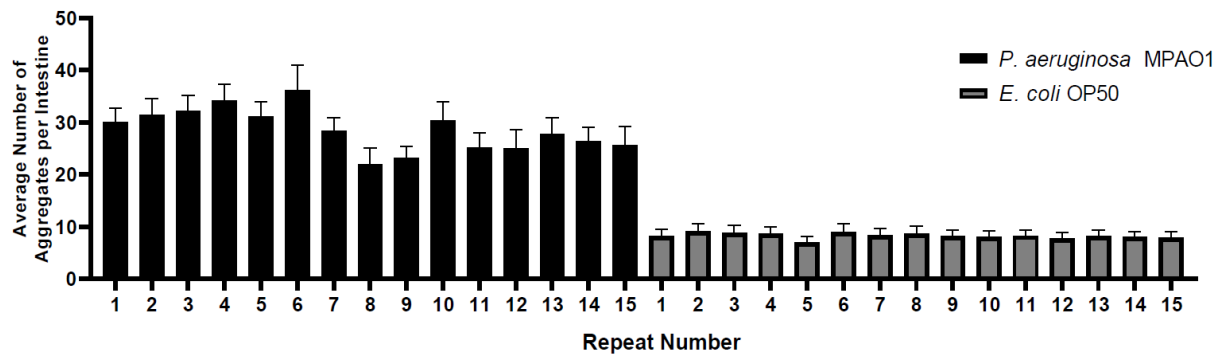
different age. Additionally, most results are expressed as a percentage of worms with aggregates. We decided not to express our results as the number of worms with aggregates, because our approach provides an additional level of details (aggregates/worm). Furthermore, after prolonged culturing, the polyQ44::YFP transgene is suppressed and worms no longer express fluorescence (or very dim non-aggregating). As soon as we see this, we thaw fresh worms. However, when we compare the general aggregation trend (i.e., OP50 vs PAO1 or aging), our data agree with previously published results. One study by Kumsta et al. observed ~15 polyQ44 aggregates per intestine in day 5 worms fed *E. coli* expressing empty vector RNAi. Our counts are performed around the same time and we get ~10 aggregates per intestine of worms fed *E. coli* OP50.

To further address this concern in the manuscript, we have added lines 744-749.

Second, they need to show how reproducible the method is - would quantifying the same well of worms several times, while agitating the animals in between measurements to make them 'change position', give consistent counts?

#### Response:

We thank the reviewer for this great suggestion. As advised, we acquired 15 images of 15 worms with agitation between each acquisition. The rationale for this experiment was to determine the consistency of aggregate quantification if worms are positioned differently within the well. This experiment was performed using both *P. aeruginosa* MPAO1 and *E. coli* OP50. We found no statistically significant differences in the average number of aggregates per intestine across the 15 images. We have added Supplemental Figure 3 (see below) and the corresponding text (lines 519-525).



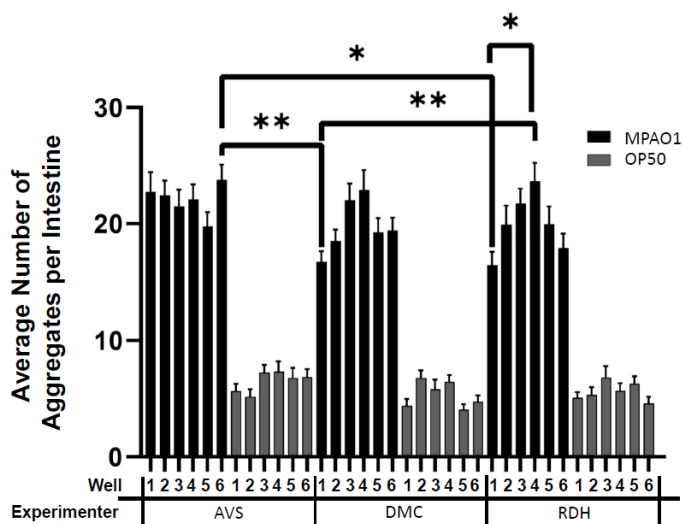
Would several wells started from the same population give the same reading?

Would processing by different people from the same worm population give comparable results (since one of the main arguments seems to be removal of bias)? The different trials in Fig 4A address a different aspect of reproducibility and does not explicitly address the above points

## Response:

Thank you for these suggestions. We had three individuals acquire image data from 12 different wells: worms fed *P. aeruginosa* MPAO1 (six wells) and *E. coli* OP50 (six wells). It is important to note that two of the individuals never used this method before. Each experimenter acquired images of worms from each well and the images were subjected to CellProfiler analysis. The results show that none of the 18 samples that were fed *E. coli* OP50 had a statistically different aggregation count, which indicates superior reproducibility. However, we did detect a few significant differences in aggregation in worms colonized by *P. aeruginosa* MPAO1 between 4/18 samples. Collectively, these results emphasize the ease and reproducibility of this method. This experiment also addresses the reviewer's question on technical replicates.

We have added Supplemental Figure 2 (see below) and text (lines 507-517) to the manuscript.



2. The paper is confusing in its balance of experiments and discussion - the discussion seems heavily focused on the impact of growth conditions like temperature or worm density on aggregation, but no data are presented on these points. While emphasizing the environmental effects on proteostasis and protein aggregation is important, it needs to be supported by data. As just one example, the authors grow worms at 25C instead of the usual 20C, and state in the discussion that they observed the effect of temperature changes on aggregation, but do not show any data.

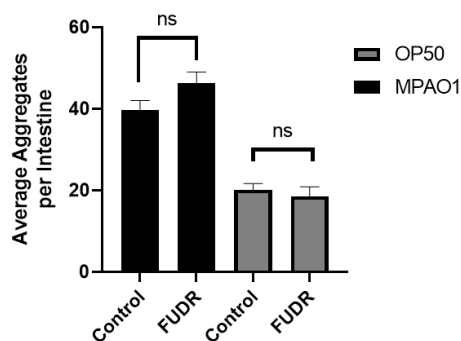
**Response:**

We thank the reviewer for this feedback and have modified the discussion section.

Similarly, how does inclusion of FUDR affect their results? To my knowledge, exposure to FUDR during development is toxic to worms, and have also been shown to induce the heat shock response. Either showing missing data or re-working the focus of the discussion (and also clearly stating that the growth conditions are not evaluated in this paper) would be acceptable.

**Response:**

Thank you for pointing this out. It was not clear from our protocol that we placed worms on FUDR after they fully developed into young adults – we made this clear in a Note (line 125-128). Also, we added extra clarification in the discussion (lines 713-720). Finally, we showed that FUDR does not affect intestinal polyQ aggregation under our experimental conditions (Supplemental Figure 5, see below).



Conversely, while the imaging and the data processing pipeline are the core of the new methodology presented here, no discussion of their strength and weaknesses is given. Some of the issues that need to be discussed may be the same as 5 mentioned above (detecting aggregates of different sizes, overlapping ones, etc.).

**Response:**

We have extended the discussion to cover strengths and weaknesses.

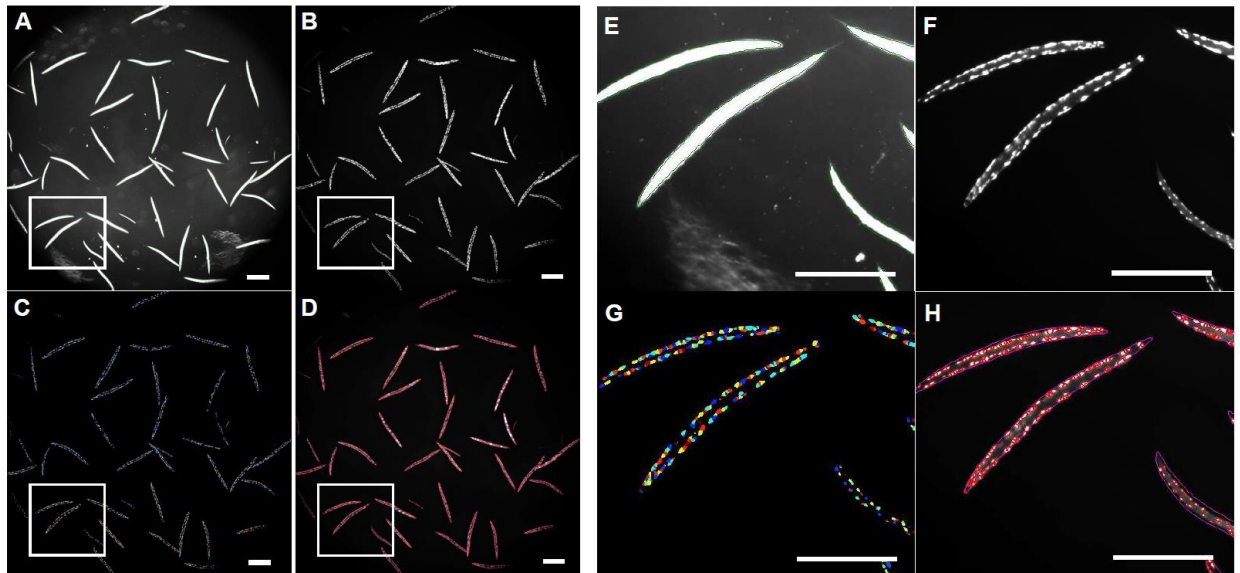
Some of the other issues that need to be discussed (or perhaps the authors have experimental data) are: would freezing step affect unstructured aggregates or is this pipeline specific to polyQ aggregation or perhaps other amyloid-like aggregates; would this pipeline work for

aggregates that are, unlike the intestinal ones, not in the same focal plane, such as muscle or neuronal ones; etc. If no, perhaps the title and abstract should reflect that.

**Response:**

We thank the reviewer for these additional suggestions/questions. We have only tested the effect of freezing using intestinal and muscle polyQ. The effect of freezing on other models is not known. We have addressed this in lines 722-727.

We also report that this pipeline may be used to identify muscle polyQ aggregates (new Supplemental Figure 1, see below); however, further modification is required and is not supported by the current version of the protocol (addressed in lines 456-463). In the previous comment (Reviewer 1), we emphasized that quantification of muscle polyQ aggregates will require additional optimization to determine the best polyQ length, age of worms, and exposure time. Also, magnification will have to be optimized to maximize the detection of aggregates that are located in a different focal plane. We believe these optimizations would make the submitted manuscript too extensive. We have not explored the application of our approach using neuronal polyQ; however, our approach will most likely be feasible but will require the acquisition of images at higher resolution and magnification, which will affect throughput



Finally, the discussion has some odd statements, like 'The inclusion of the OP50 control will ensure that the ratio of the number of aggregates between the control and the experimental group is conserved' - this makes sense for the author's specific application of studying the effects of different food on aggregation, but not for any general application. A discussion that is geared to a more general application/usefulness of the method is needed.

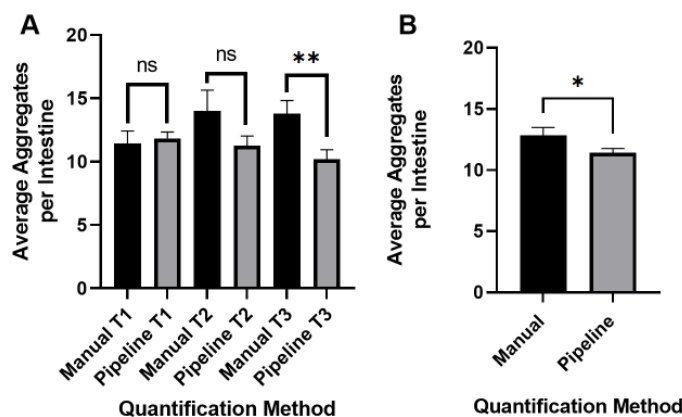
**Response:**

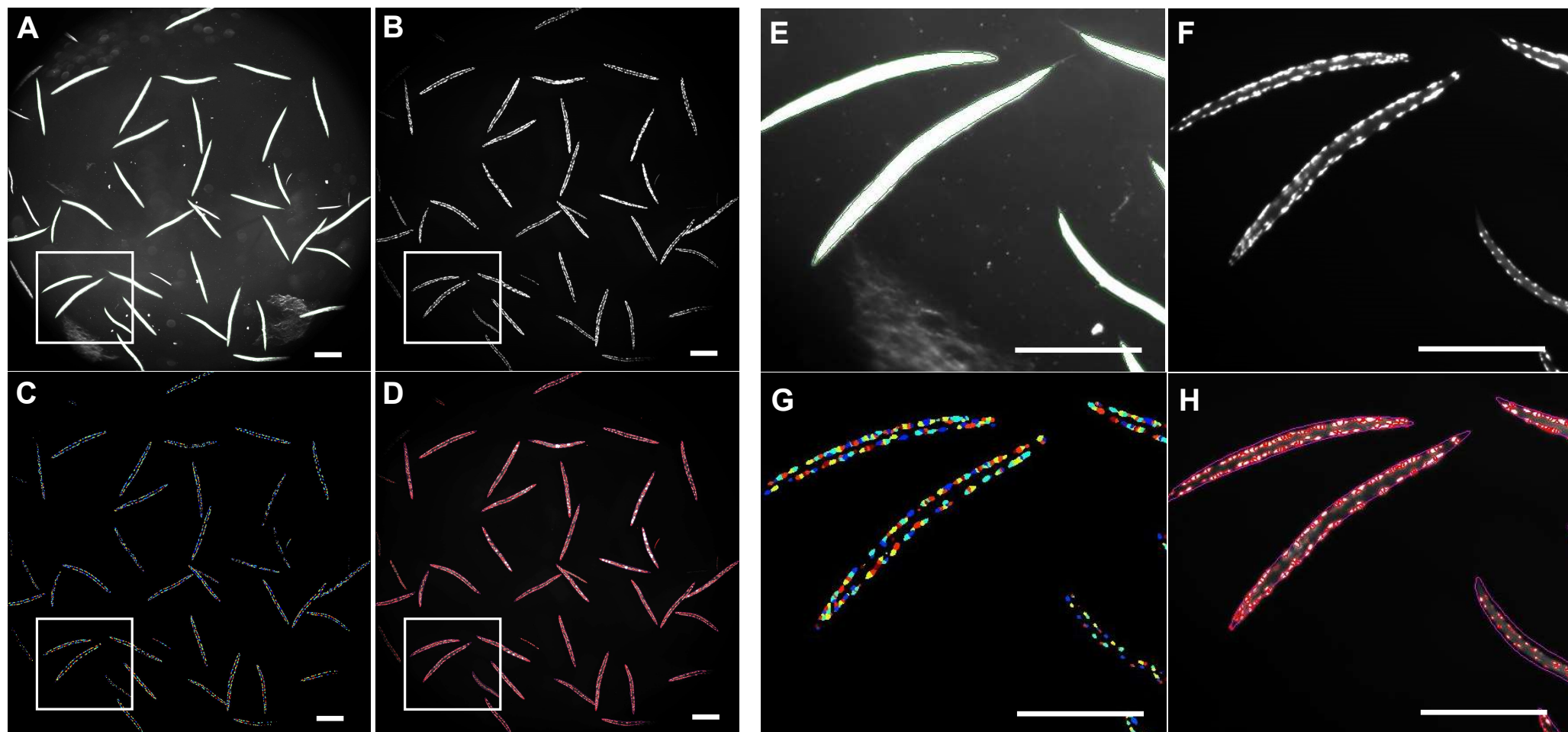
We have addressed the reviewer's concern and rewrote the discussion section to be more inclusive of potential applications (lines 777-786).

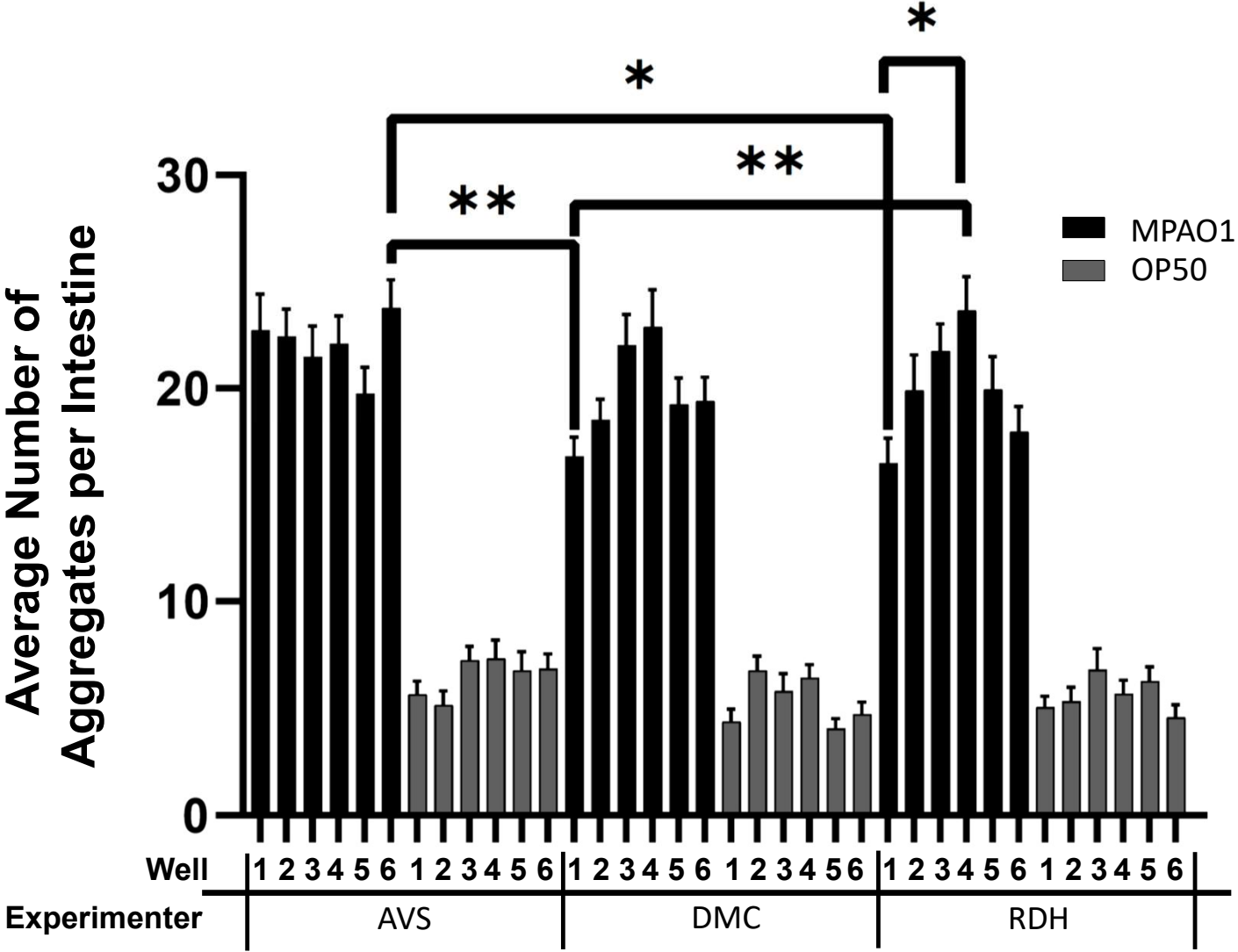
3. The variability in aggregate counts in Fig. 4A is concerning, especially since data shown are normalized to the manual counts in each trial and thus do not give any information on consistency of counts between the three trials. The actual aggregate counts, rather than relative number, will also point to where this variability comes from - are the manual counts inconsistent or the pipeline ones? As such, a nearly 20% discrepancy is a very significant one, and the authors should provide a careful discussion of potential causes, and of implications for the use of the method.

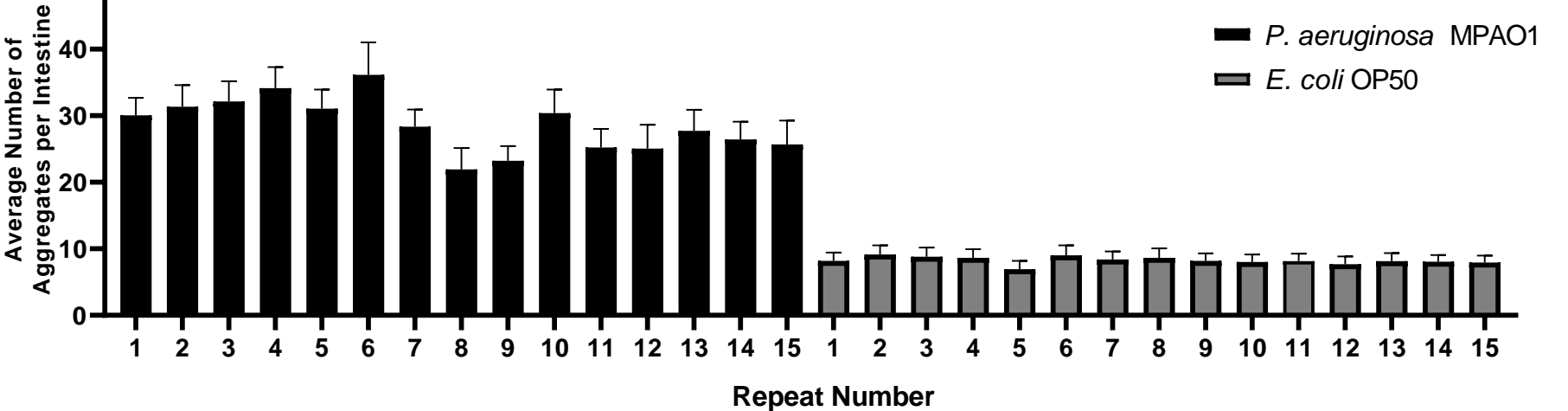
**Response:**

We have changed Figure 5 (old Fig 4) to represent the actual aggregate counts. As predicted, there is more variability in manual counts. We further address this discrepancy in the discussion section (lines 729-742).

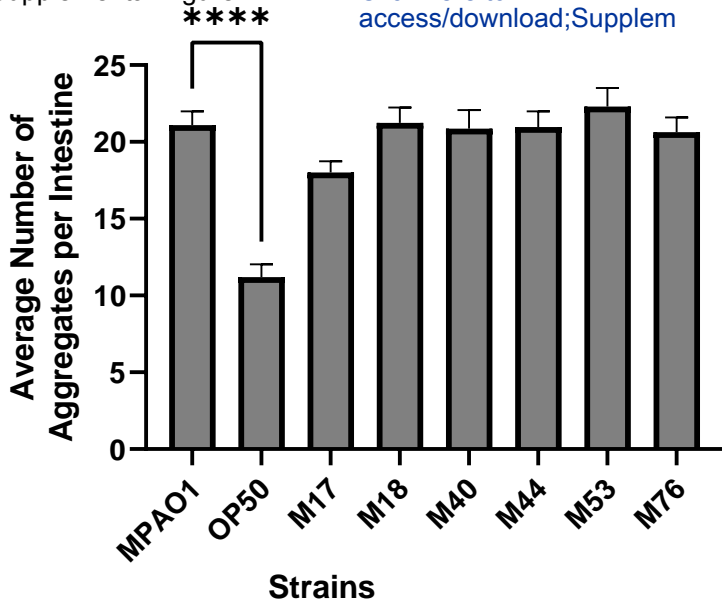


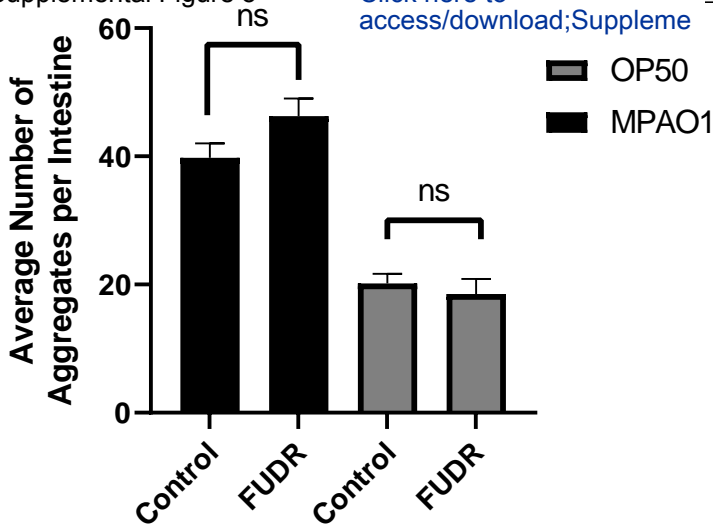






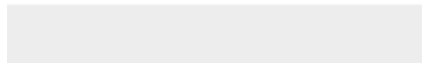


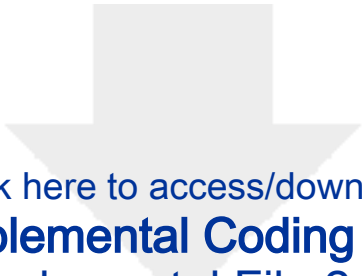




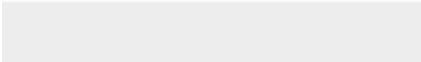


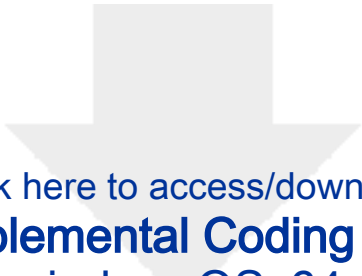
Click here to access/download  
**Supplemental Coding Files**  
Supplemental File 1.cppipe





Click here to access/download  
**Supplemental Coding Files**  
Supplemental File 2.xml





Click here to access/download  
**Supplemental Coding Files**  
gui\_windowsOS\_64x.zip

